MODELING OF STRAIN RATE EFFECTS

ON CLAYS IN SIMPLE SHEAR

A Thesis

by

BYOUNG CHAN JUNG

Submitted to the Office of Graduate Studies of
Texas A&M University
in partial fulfillment of the requirements for the degree of

MASTER OF SCIENCE

May 2005

Major Subject: Civil Engineering

MODELING OF STRAIN RATE EFFECTS

ON CLAYS IN SIMPLE SHEAR

A Thesis

by

BYOUNG CHAN JUNG

Submitted to Texas A&M University
in partial fulfillment of the requirements
for the degree of

MASTER OF SCIENCE

Approved as to style and content by:

Giovanna Biscontin (Chair of Committee)	James D. Murff (Member)
Christopher C. Mathewson (Member)	David V. Rosowsky (Head of Department)

May 2005

Major Subject: Civil Engineering

ABSTRACT

Modeling of Strain Rate Effects

on Clays in Simple Shear. (May 2005)

Byoung Chan Jung, B.S., Tae Jeon University

Chair of Advisory Committee: Dr. Giovanna Biscontin

The objective of this research is the development of a new constitutive model to describe the behavior of cohesive soils under time dependent loading. In the work presented here, the modified SIMPLE DSS model is expanded to account for the effects of strain rate on clays in simple shear conditions. The response of clay soils is highly dependent on the rate of strain for both effective stress path and stress-strain behavior. The undrained shear strength is strongly influenced by strain rate both in monotonic and cyclic simple shear tests. Nevertheless, the few available experimental results cover a very limited range of loading conditions and rates. The existing literature established that the soil response display a unique relationship between shear strength and log scale of strain rate. To include the effects of strain rate, the modified simple effective stress model starts with two assumptions: (1) a specific shear strength corresponds to a specific strain rate in a unique relation; and (2) the effect of strain rate does not change the failure envelope. The proposed model is developed from the original SIMPLE DSS model, based on an effective stress formulation in a reduced stress space, and utilizing concepts related to the framework of bounding surface plasticity. The proposed model evaluation was carried out comparing model simulations with results of simple shear tests on Boston Blue Clay and San Francisco Young Bay Mud. The model capability is useful especially in strain rate dependent responses for both monotonic and cyclic behavior, including irregular loading and step-changed condition. It was found that undrained shear strength in simple shear is directly related to strain rate effects and the responses in cyclic test show the more rate dependent behavior than those in monotonic test. The proposed model is able to predict the increase in undrained shear strength for higher strain rate.

ACKNOWLEDGMENTS

First, I owe to my most sincere gratitude to God.

I would like to express deepest gratitude to my advisor, Dr. Giovanna Biscontin, for the encouragement, valuable suggestions, challenges, and patience on this work.

I would like to also thank Dr. James D. Murff and Dr. Christopher C. Mathewson for serving as the advisory committee at the final exam.

I want to thank my many friends in this town for providing wonderful times and refreshment. Many thanks to Dr. Shin's family for their love during this research. I sincerely wish them all successful and happy lives.

In addition, I greatly acknowledge the support and endless encouragement of my family, who always showed open hearts and supported me unconditionally over the past several years of this work.

Finally, I take this opportunity to thank my wife, Jung Mi Do, and super cute daughter, Ellie Esther Jung, for their trust, understanding, and patience during this demanding part of my life. Especially, this thesis is dedicated to my parents and grandmother, Sun Ho Kim, Soon Tae Jung, Hae Bok Lee, and Jung Sook Song.

TABLE OF CONTENTS

LIST OF FIGURES

FIGURE Page

LIST OF TABLES

CHAPTER I

INTRODUCTION

1.1 GENERAL

Any material subjected to continuous loading will deform and fail. In geotechnical engineering, the response of saturated soil has a very important role in the stability of submerged slopes. Because the behavior of soil in real conditions is quite complex it is too hard to predict exactly. In the case of saturated clay, the behavior of soil can be affected by various factors including the pore pressure, the effective stress, loading path, and the history of loading. The response of clay soils is highly dependent on the rate of straining and loading for both effective stress path and stress-strain behavior. The early works of rate effects in terms of the soil strength were summarized by Housel (1960). The early investigations revealed that the strength increases as the rate of straining increases. The larger shear resistance at larger strain rates results from characteristic of viscous materials because soils behave like a viscous fluid and a more viscous material allows the larger resistance under same shear stress (Matesic and Vucetic, 2003).

To obtain a realistic for time dependent problems, it is essential to use a model that accounts for rate effects in the stress-strain-strength properties of soils.

This thesis follows the style and format of the *Journal of Geotechnical and Geoenviromental Engineering*.

The stress-strain-strength behavior of soils is known to be time and history dependent, and will therefore be different between isotropic and anisotropic consolidation. The time dependant deformation of a soil has two components, the elastic and plastic. Several types of laboratory test are performed to define and simulate the field behavior of saturated clays subjected to cyclic and monotonic loading, and estimate various soil parameters. In this work, I will mainly concentrate on the direct simple shear test. The direct simple shear test can represent the actual stress conditions in a number of problems, including marine slopes. Also, most of the constitutive models for soils have been developed extensively for triaxial and direct simple shear tests. Because of the significant influence of strain-rate on clay behavior, modeling needs to address that issue. The new predicting model is illustrated through parameter investigation and comparison with a limited number of existing tested data.

1.2 SCOPE OF WORK

The modeling of the effect of strain rate on the response of a cohesive material upon being subjected to monotonic and cyclic loading conditions is the focus of this research work. A review of previous work on the effect of strain rate is also carried out. In the same way, Biscontin's (2001) dissertation on direct simple shear for the experimental analysis and modeling of San Francisco Young Bay Mud with SIMPLE DSS model is reviewed.

This research focuses on modeling of strain rate effects for the soil response in simple shear. The research work is divided into three parts:

1. **Development of relationship (strength-strain rate)**: the relationships between undraind shear strength and strain rate are in the literature reviews studied to describe the unique characteristics in soil response.

2. **Model development**: the modified SIMPLE DSS model base on the SIMPLE DSS includes the effects of strain rate in simple shear.

3. **Model evaluation**: performance of verification is conducted by comparing the model prediction with measured response.

1.3 THESIS CONTENT

A brief description of the organization of the chapters that form this thesis follows:

Chapter II provides a summary of previous work reviewed for this investigation in the area of the effect of strain rate including experimental results and modeling of soil response.

Chapter III presents a review of experimental results for direct simple shear on Young Bay Mud performed by Biscontin (2001).

Chapter IV presents a detailed description of the modified SIMPLE DSS model based on Pestana et al. (2000).

Chapter V presents model analysis of the behavior both monotonic and cyclic test. In addition, it presents the results of the comparison between the experimental and computational analysis.

Finally, Chapter VI presents summary, conclusions, and recommendations for future research.

CHAPTER II

LITERATURE REVIEW

2.1 INTRODUCTION

Any material subjected to continuous loading will deform and fail. In geotechnical engineering, the response of saturated soil has a very important role in the stability of submerged slope. Because the behavior of soil in real conditions is quite complex it is too hard to predict exactly. In the case of saturated clay, the behavior of soil can be affected by various factors including the pore pressure, the effective stress, and the history of loading condition. The shear strength of soils has been one of the most intensively investigated by numerous researchers. The shear strengths were defined by the maximum deviatoric stress and shear stress level for triaxial test and simple shear respectively. Early investigations on cohesive soils were focus on conducting experimental work mainly triaxial test. This chapter summarizes some of the previous experimental research work into the effects of strain rate on shear strength and stress-strain behavior of cohesive soils for both monotonic and cyclic tests. Some experimental and modeling results suggested by some of investigators are also reviewed.

2.2 SIMPLE SHEAR CONDITION

This research focuses on the simple shear condition as part of a border study on the response of submarine slopes. Therefore, the simple shear mechanism should be defined. On discussing the simple shear condition, Biscontin (2001) says:

When only gravity loads are acting, a generic soil element in the slope is subjected to a stress in the direction normal to the slope, represented by the effective stress, and a stress in the plane of the slope, parallel to the dip, represented by the consolidation shear stress. For the purpose of the simulation, the earthquake motion is assumed to consist only of shear waves propagating normal to the free face of the slope. This consideration is analogous to the assumption of vertically propagating, horizontally polarized shear waves for level ground conditions. The seismic motion then results in additional cyclic shear stress acting on the plane of the slope in a direction oriented at some angle with that of the consolidation shear stress. During an earthquake the loading would be of short duration and he low hydraulic conductivity of the clayey soils would not allow dissipation of the excess pore pressure caused by the shearing. Thus, it will be assumed that undrained conditions exist in the slope during seismic loading. The state of stress applied to an element of soil in the slope can be recognized as one of simple shear. The knowledge accumulated on the behavior of soft clays in undrained conditions in simple shear can then be used to develop a constitutive law that would realistically describe the soil response.

Fig 2.1 shows the stress states in simple shear conditions.

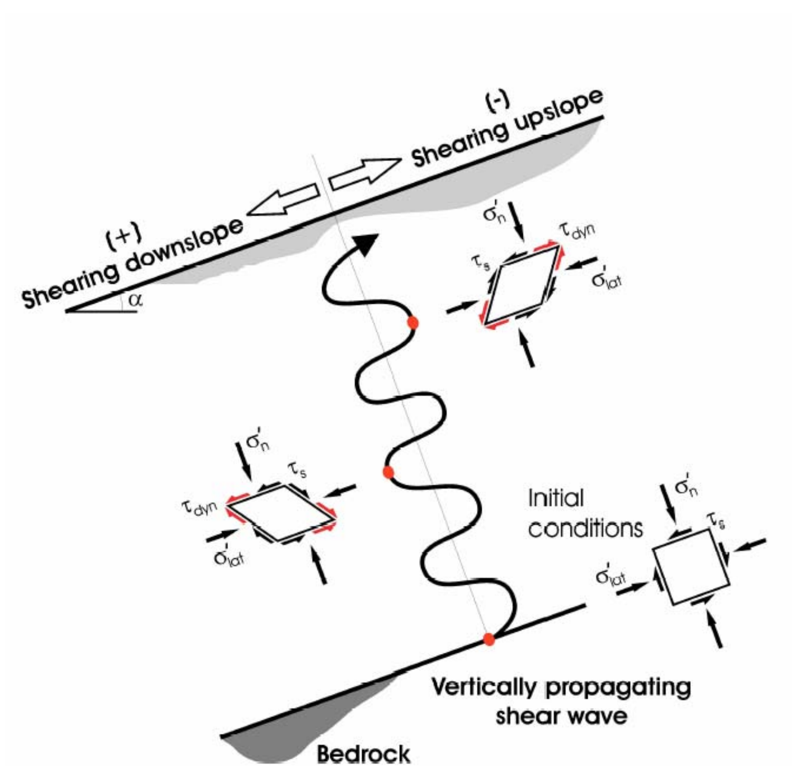

Fig. 2.1. Stress States in Simple Shear Conditions

2.3 EXPERIMENTAL REVIEW

Housel (1960) reviewed the all of early work on the rate effects on cohesive soil researched until 1958 in an ASTM Special Technical Publication. His work contains many observations of the effect of rate on shear strength in ring shear, unconfined compression, direct shear box, vane shear, and triaxial tests. From the review of the available experimental work, he derived additional conclusions in his paper. The effect of rate of loading on plastic soils was recognized that the rapid rates of loading increased resistance. Then, he suggested that:

"The effect of rate of loading must be tested at several rates of deformation and then be extrapolated back to zero rates to determine the static resistance."

Perloff (1962) also summarized the early accounts of the effect of rate of testing on shear strength in his Ph.D dissertation. He performed laboratory experiments to define the relationship among strength, stress history, and strain rate in consolidated-undrained triaxial compression test at several strain rates on remolded clay samples with varied stress histories. Fig. 2.2 shows the effect of strain rate on strength parameter $(\sigma_1 - \sigma_3)/\sigma_c$. The strength parameter decreases as the strain rate decrease, and this effects becomes more well defined as overconsolidation ratio (σ_p / σ_c) increases. Finally, Perloff (1962) suggested two future works to effect of strain rate. "Determination of the effect of strain rate on the relationships between stress history constants and the classification properties and investigation of the varying strain rates above and below the range investigated."

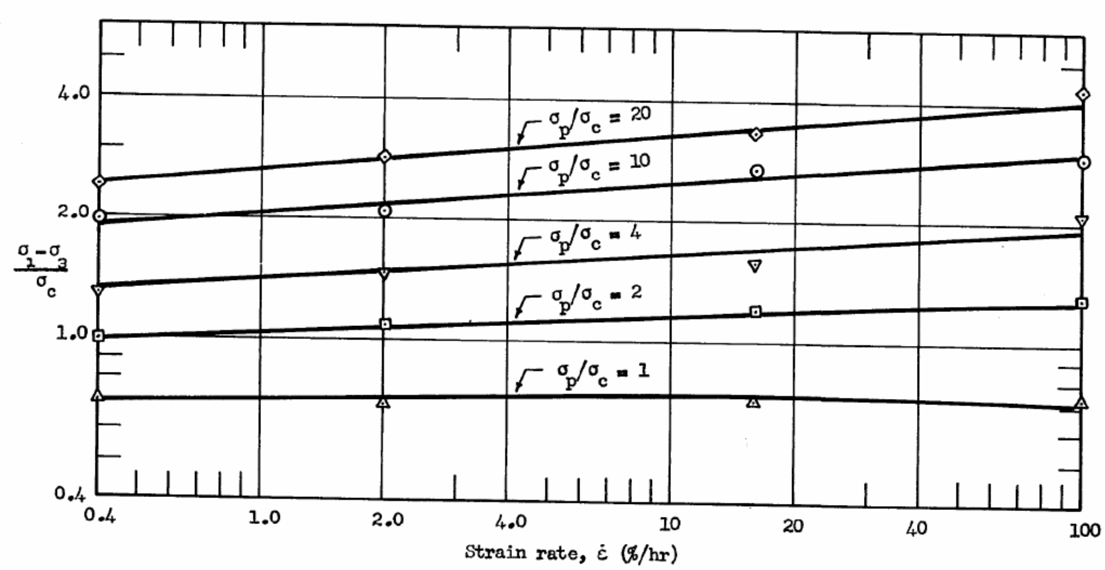

Fig. 2.2. Effect of Strain Rate on Strength (Perloff, 1962)

Richardson and Whitman (1963) introduced a novel testing known as step-changed method to study the effect of strain rate on the undrained shear strength. The strain rate is step-changed during the test performed by Graham et al. (1983) (see Fig. 2.3). For varying strain rate, the stress-strain curve follows a "pre-determined" path. So, it seems to confirm that there is a unique relation between strain rate and a corresponding stress-strain. Also, this relationship does not seems to be affected by history, sine the stress-strain curve seems to go back to the unique trace for a certain rate as the rate is changed during test. Step changing can also apply to other tests such as triaxial extension and direct simple shear test. Graham et al. (1983) proposed a strain-rate parameter, $\rho_{0.1}$, expressed as a percentage of the shear strength measured at 0.1%/hr of strain rate to represent the change in shear strength with strain rate. Graham et al. (1983) concluded that undrained shear strengths change by about 10-20% for a tenfold

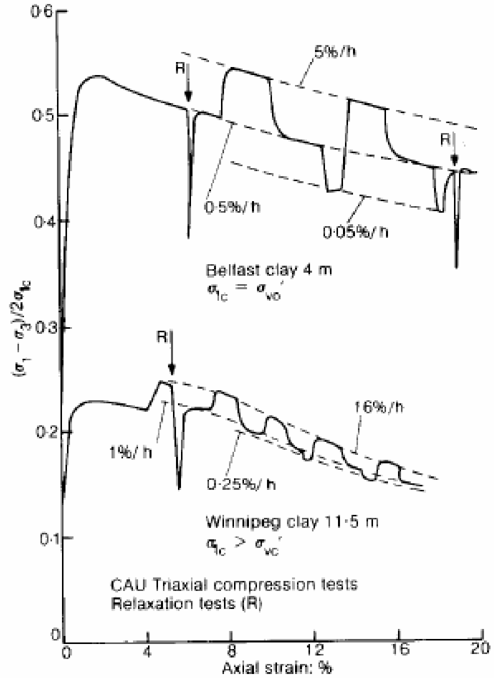

(a) Triaxial Compression Tests

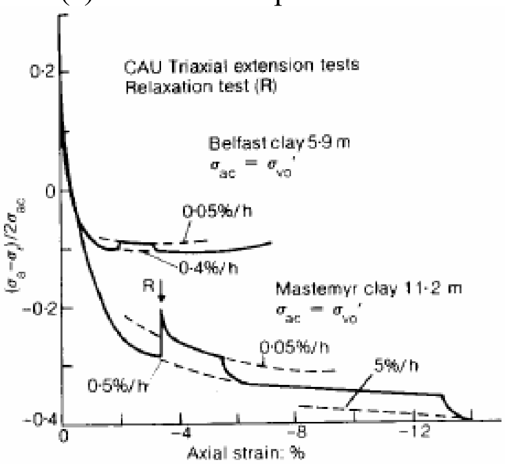

(b) Triaxial Extension Tests

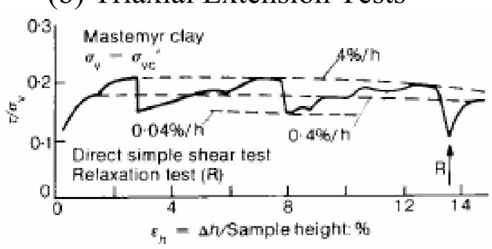

(c) Direct Simple Shear Tests

Fig. 2.3. Stress-Strain Curves with Step-Changed Strain Rate (Graham et al., 1983)

change in rate of strain for all types of soils, and is independent of plasticity, consolidation stress ratio, and stress level.

Mayne (1985) compared the shear strength between direct simple shear (DSS) and triaxial shear tests. The theoretical shear strength in undrained DSS proposed by Prevost (1979) observed that the DSS strength is an intermediate strength comparing with triaxial compression and extension test. Mayne (1985) contained the normally consolidated and over consolidated data in his paper. In undrained strength analysis, Mayne (1985) concluded that normally consolidated shear strength in DSS is about 70% of shear strength of triaxial compression test while the increasing rate in the normalized shear strength has the same rate as in triaxial compression.

Lefebvre and LeBoeuf (1987) conducted series of monotonic and cyclic triaxial tests to describe the effect of the strain rate and load cycles on the undrained shear strength of sensitive clay.

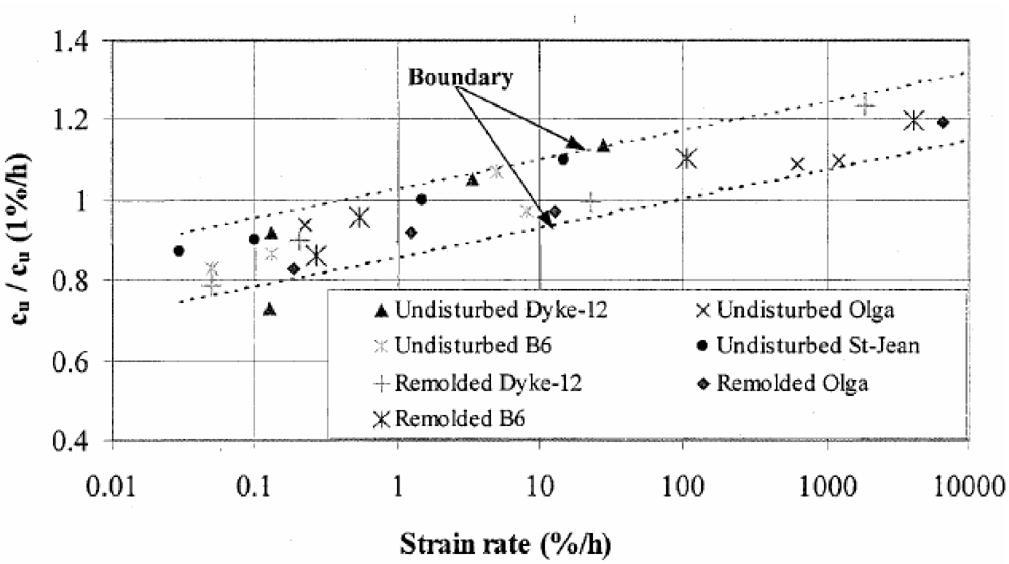

Fig. 2.4. Normalized Shear Strength Ratio versus Strain Rate
(Lefebvre and LeBoeuf, 1987)

Fig 2.4 shows the undrained shear strength measured for undisturbed and remolded samples at the different rates of strain, normalized by the undrained shear strength measured at a strain rate of 1%/hr and plotted against the log of the strain rate. These data showed a very narrow range. Furthermore, this study described the linear relationship between log of strain rate and undrained shear strength for both undisturbed and remolded samples.

Andersen (1991) addressed the soil testing model which takes into account the complexity of stress conditions in soil under structure subjected to a combination of static and dynamic load in the book of cyclic loading of soils edited by Reilly and Brown.

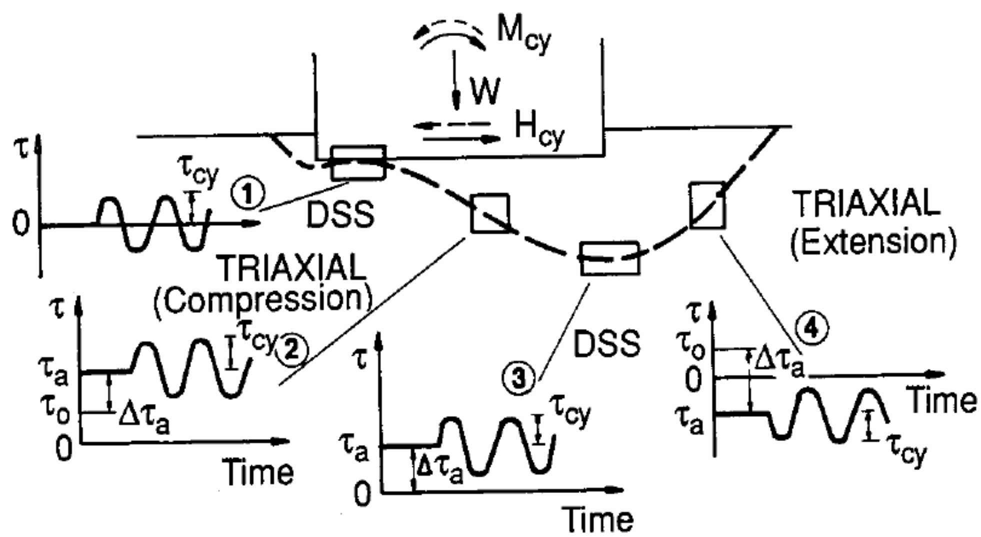

Fig. 2.5. Example of Tests along the Failure Plane (Andersen, 1991)

Fig. 2.5 shows an example of test model conditions for different soil elements along the potential failure plane. Schematic loading time histories for each of the elements, subjected to different loading, combining an average shear stress with cyclic shear stresses. The average shear stresses are the combination of an initial static shear stress, for example due to sloping ground, and an additional shear stress under structure. For element 1 and 3, the only horizontal forces will be composed at surface and the shear will be horizontal. This represents a direct simple shear stress (DSS) condition. Otherwise, compression and extension forces will be applied to element 2 and 4 respectively. Therefore, element 2 is best represented by the triaxial compression test and element 4 is best represented by the triaxial extension test. This example shows that triaxial and direct simple shear tests should be performed in the laboratory test program to fully characterize the response of the soil on the failure surface.

Sheahan et al. (1996) conducted 25 K_0 consolidated triaxial compression test on residemented Boston Blue Clay with overconsolidation ratio (OCR) varying from 1 to 8 and several axial strain rates (0.05%, 0.5%, 5%, and 50%/hr). They conclude that the effective stress envelopes at maximum shear stress are dependent of strain rate in triaxial compression tests. They introduced the general rate sensitivity parameter, $\rho_{\dot{\varepsilon}_{a0}}$.

$$\rho_{\dot{\varepsilon}_{a0}}(\%) = \left[\left(\Delta s_u / s_{u0} \right) / \Delta \log \dot{\varepsilon}_a \right] \times 100 \tag{2.1}$$

Where,

$\dot{\varepsilon}_a$ = range of strain rates

s_{u0} = value of s_u at the reference strain rate, $\dot{\varepsilon}_{a0}$.

They described that "$\rho_{\dot{\varepsilon}_{a0}}$ can change with both the strain rate range tested and OCR." They also found the amount of variation at different strain rates for the four

OCRs tested. Fig. 2.6 shows the experimental results of their work with varying strain rate at OCR=1. The study indicated that the peak shear stress increases consistently with increasing strain rate and the changing of strain rate affects strain softening. However, the shape of the normalized shear-induced pore pressure versus axial shear strain indicate a lesser generation of pore pressure when strain rate increased as shown in Fig. 2.7.

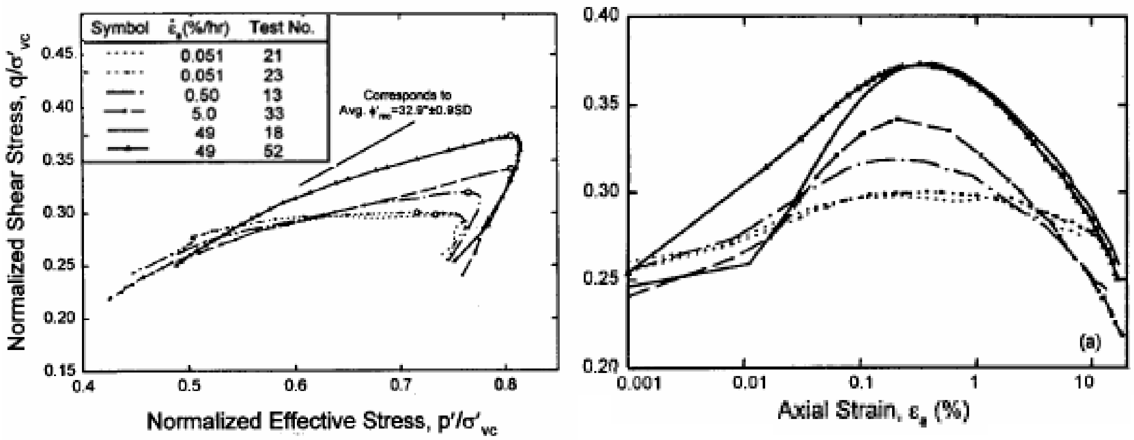

Fig. 2.6. Normalized Effective Stress Path and Shear Stress-Strain Behavior, OCR=1 CK_0UC Test on Resedimented BBC (Sheahan et al., 1996)

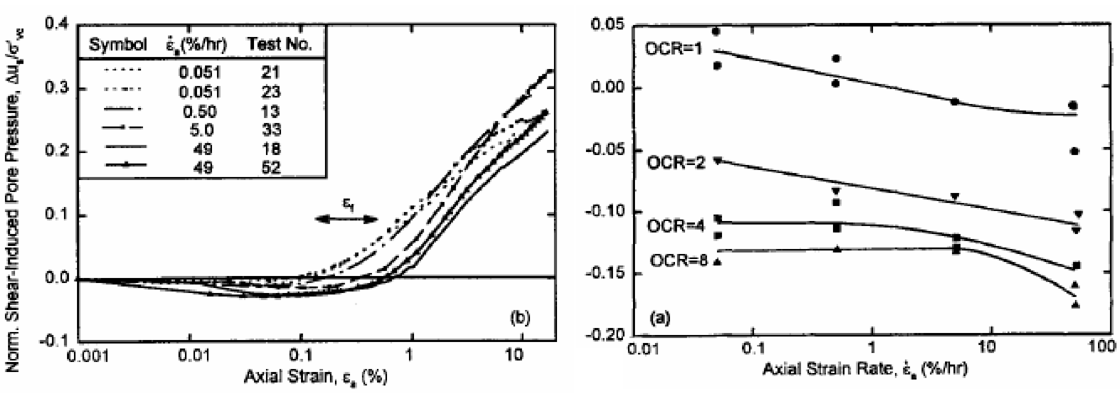

Fig.2.7. Pore Pressure versus Axial Strain Behavior (Sheahan et al., 1996)

Awoleye et al. (1991) performed unconfined compression test, with a normally consolidated soft to medium silty clay. They recognized the effects of duration and rate of loading on the unconfined compression test. They reported the results of testes performed on highly plastic clay with three strain rates, fast, medium, and slow, for both the remolded and undisturbed clay soil in unconfined compression tests. “An increase in strength due to an increase in the strain rate is observed in the unconfined compression test on the triaxial equipment.” Remolded clay typically becomes softer than it was when undisturbed because of breaking of the structure. “The increase in strength of undisturbed samples due to an increase in rate of strain was more than the increase in remolded strength. Hence, the sensitivity increases with the rate of strain (Fig. 2.8).”

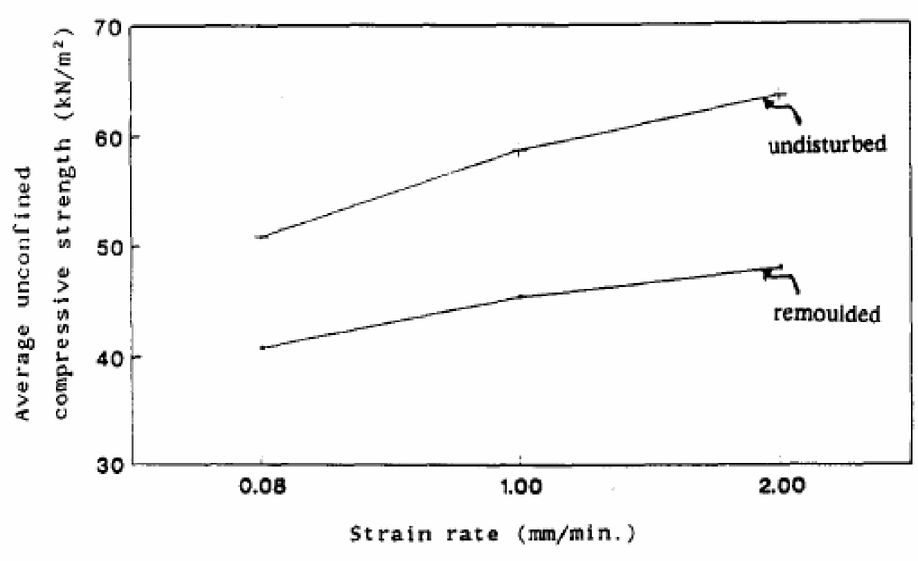

Fig. 2.8. Average Unconfined Compressive Strength versus Strain
(Awoleye et al., 1991)

Similarly, Zhu and Yin (2002) and Katti et al. (2003) proposed the same conclusion that the shear strength response at peak shear stress follows a linear function of change in OCR with increasing strain rate in Hong Kong Marine Clay (HKMC) and Resedimented Boston Blue Clay (BBC), respectively, as shown in Fig.2.9.

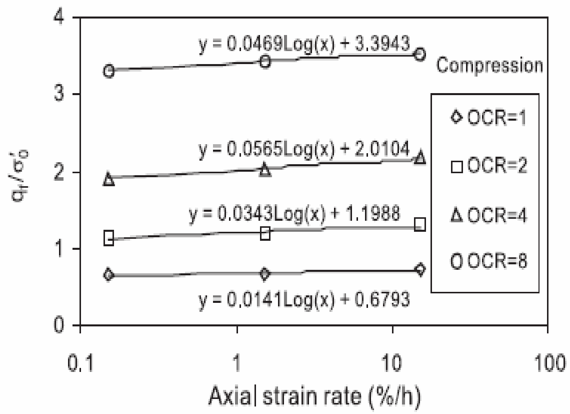

(a) HKMC (Zhu and Yin, 2002)

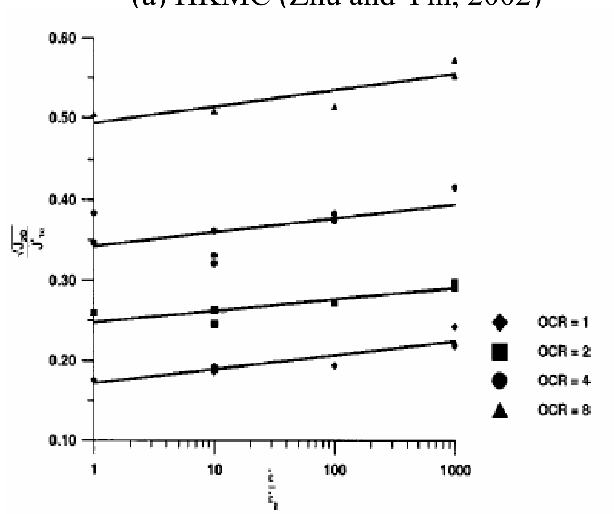

(b) Resedimented BBC (Katti et al., 2003)

Fig. 2.9. Normalized Shear Strength versus Strain Rate

2.4 MODELING REVIEW

Luccioni (1999) presents model prediction for lightly overconsolidated clay based on the triaxial testing. In his work, a new rate independent constitutive numerical model is proposed and validated with both drained and undrained triaxial and plane strain tests. The model referred to as Bear-Clay model, is based on the incrementally lineralized theory of plasticity. The Bear-Clay model needs nine input parameters to predict the soil behavior. Among these nine parameters, the first five input parameters can be obtained from direct laboratory testing, while the other four parameters can be determined by parametric studies using testing data. Bear-Clay model formulation can capture a variety of features using a versatile yield surface, small-strain non-linearity, and evolving anisotropy shear strain response. Table 2.1 shows the overall Bear-Clay model input parameters.

Table 2.1. Summary of Bear-Clay Input Parameters

<table>
<tr><th>Input Parameters</th><th>Effect of Predicted response</th><th>Determination of Prameters</th></tr>
<tr><td>ρ_c</td><td>Describe the slope of LCC</td><td>Hydrostatic or 1-D Compression test</td></tr>
<tr><td>ρ_{ro}</td><td>Controls the amount of Non-linearty in volume</td><td>Hydrostatic or 1-D Compression test</td></tr>
<tr><td>μ</td><td>Average Poisson's ratio</td><td>Pressuremeter or 1-D compression with lateral stress measurement</td></tr>
<tr><td>ω_s</td><td>Describe the small strain non-linearty in shear</td><td rowspan="5">Undrained Triaxial Compression and Extension</td></tr>
<tr><td>ϕ_{cs}</td><td>Critical State friction angle</td></tr>
<tr><td>m</td><td>Describe the yield surface</td></tr>
<tr><td>β</td><td>Controls the geometrical shape of LC boundry surface</td></tr>
<tr><td>ψ</td><td>Controls the rate of change of anisotropy</td></tr>
<tr><td>G_b</td><td>Controls the small strain shear stiffness</td><td>Elastic Shear Wave velocity or small strain appratus</td></tr>
</table>

The results of his study indicate that the Bear-Clay model yielded good predictions of anisotropic shear stress-strain-strength response compared with measured data for different consolidation histories. Also, model predicts quite well the maximum shear stress condition and the nonlinear

Biscontin (2001) represents the simplified effective stress model incorporating the realistic stress-strain-strength response, initial anisotropic conditions due to slope angle, excess pore pressure generation, and accumulation of plastic strain during cyclic loading to describe the monotonic and cyclic response of cohesive clays in simple shear. The state boundary surface of the simple DSS model was modified from the Bear-Clay model for lightly overconsolidated clays (Luccioni, 1999). The concept of the formulation comes from elasto-plasticity and incorporates anisotropic hardening to control different stress and strain reversal histories.

This model represented both monotonic and cyclic behavior of slightly over consolidated clay. In this work, limited multi-directional monotonic and cyclic tests were conducted and several samples were subjected various consolidation shear stress ratios corresponding to slope angles of soil deposits. The simple DSS model needs seven input parameters to predict soil behavior in both monotonic and cyclic response. The five input parameters control mainly the monotonic behavior and two input parameters describe the response of cyclic tests. Material parameter β defines the failure ratio or the excess pore pressure at failure, and m describes the shape of plastic state surface (see Fig. 2.10).

Fig 2.10 showed that the parameter m controls both shape of the stress path and maximum undrained shear strength, while parameter, β, plays a part, but mostly controls the generation of excess pore pressure at failure. For a given m, an increase in β results

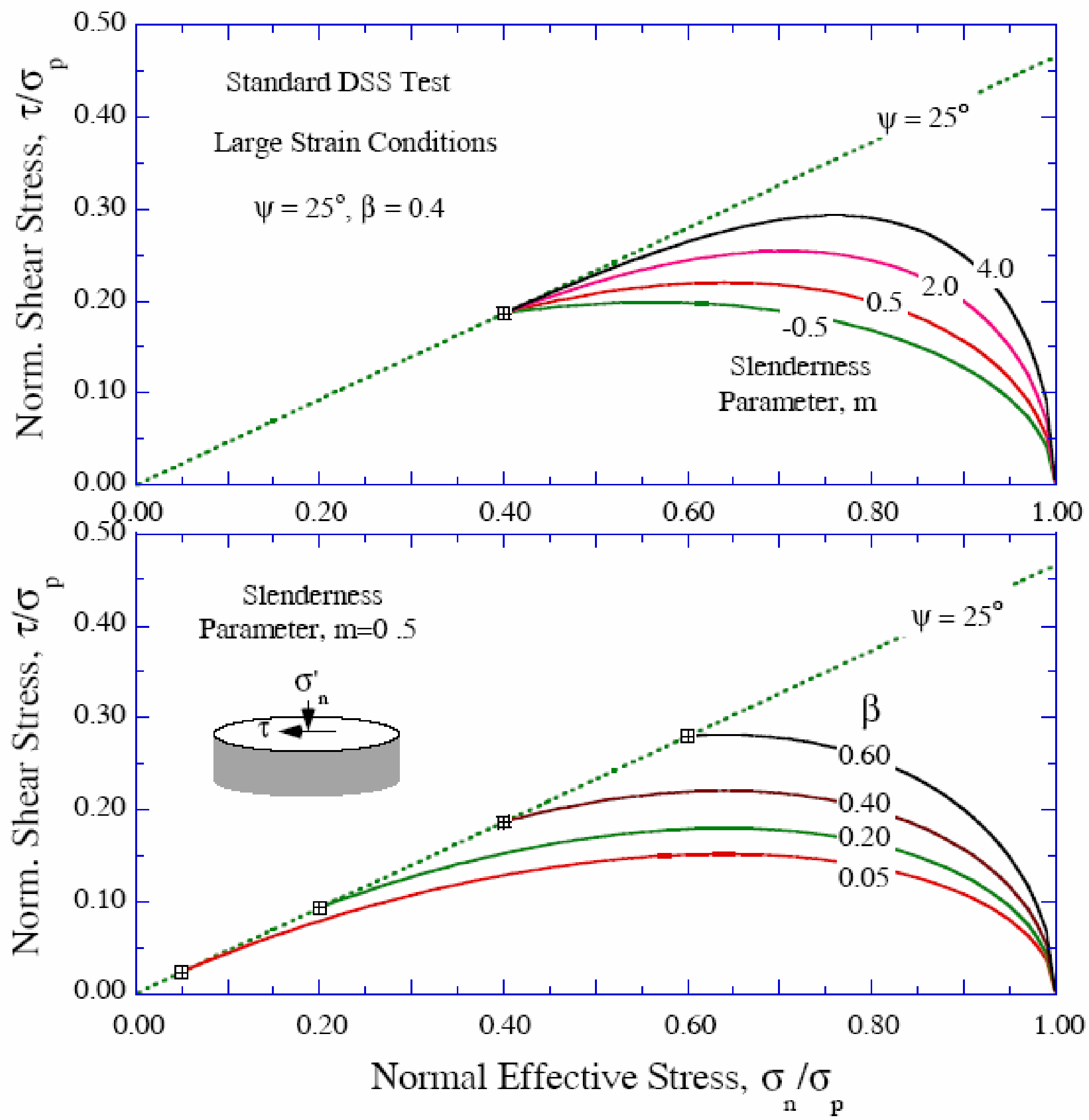

Fig. 2.10. Effect of Material Parameters (*m* and *β*) for Monotonic Test (Biscontin, 2001)

in an increase in both shear stress and undrained shear strength. However, for a given value of β, the undrained shear strength is only dependent on value of m.

Material parameter G_p captures the first loading stress-strain response for soil samples. Higher value of G_p shows stiffer response at small strains, but strain softening occurs at large strain condition (see Fig. 2.11).

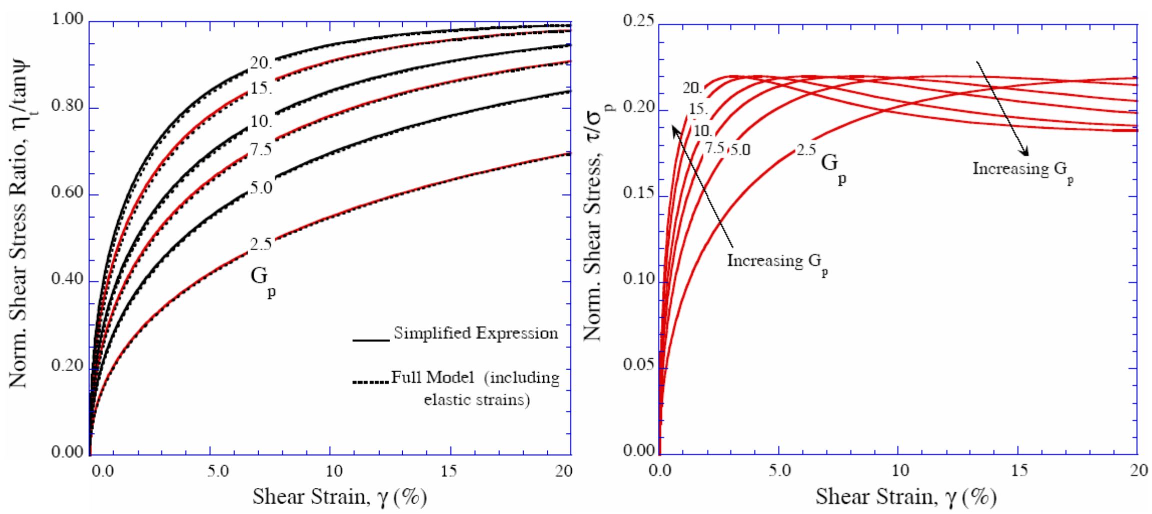

Fig. 2.11. Effect of Material Parameter (G_p) for Monotonic Test (Biscontin, 2001)

In cyclic DSS test, the effective stress is the function of material parameter θ. Therefore, θ control the both stress path and excess pore pressure generation as shown in Fig. 2.12. The lower value of material parameter θ produces the higher pore pressure generation.

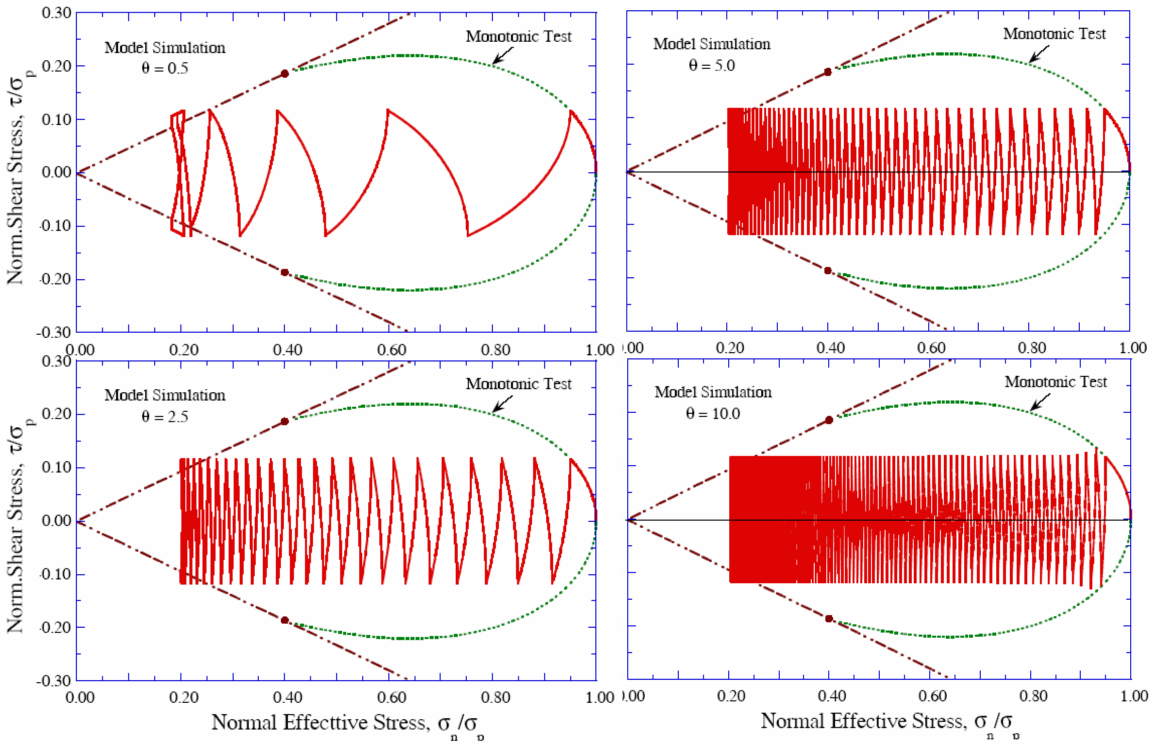

(a) Effective Stress Path

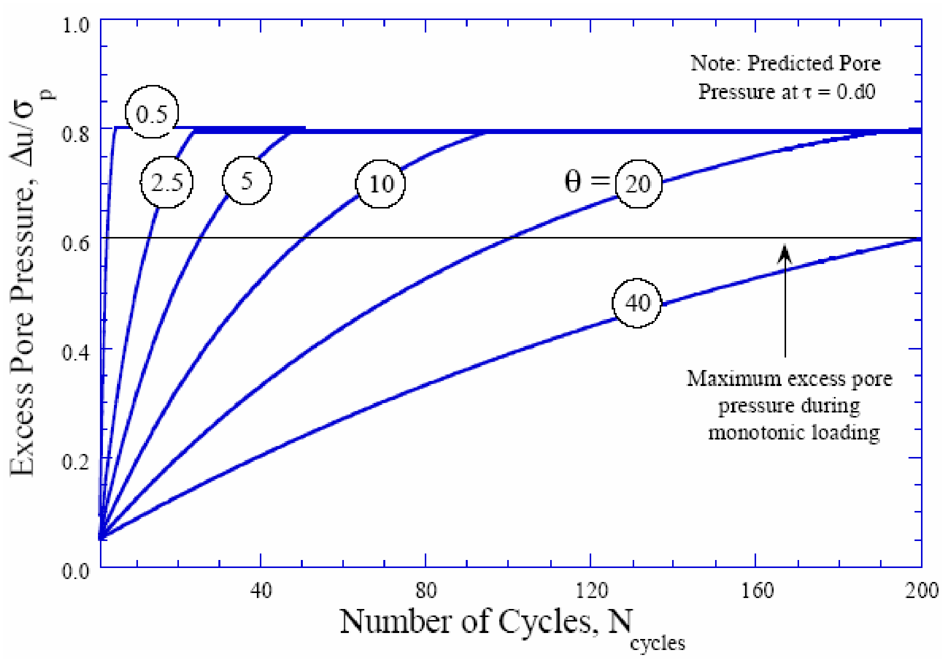

(b) Pore Pressure Generation

Fig. 2.12. Effect of Material Parameter θ for Cyclic Test (Biscontin, 2001)

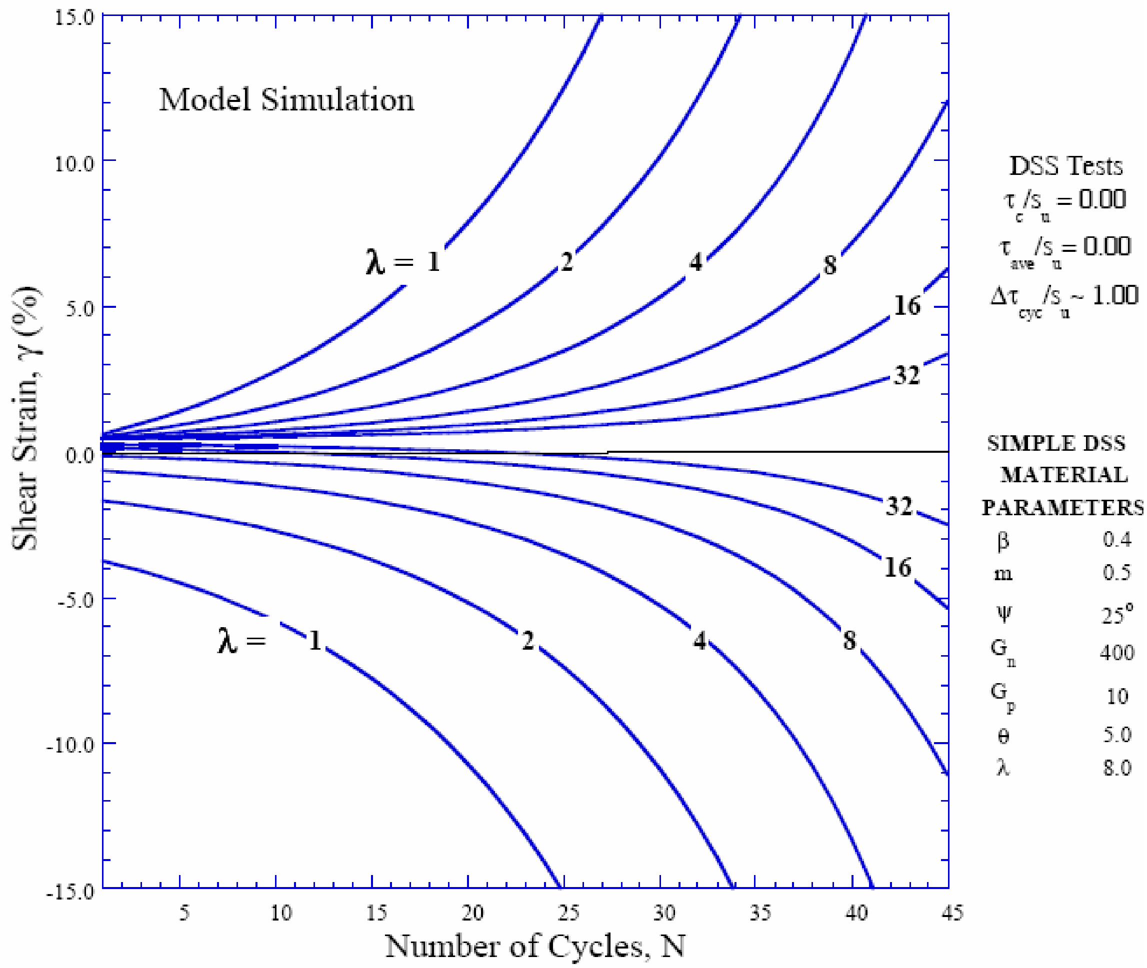

Fig. 2.13. Effect of Material Parameter λ for Cyclic Tests (Biscontin, 2001)

The increment of plastic strain is the function of parameter λ, while effective stress s the function of parameter θ. Fig. 2.13 gives the relationship between shear strain and number of cycles for cyclic test as a function of λ. The results of Simple DSS model for monotonic NC simple shear tests show good agreement with a data, including the effects of anisotropy and loading direction. Table 2.2 summarized the material input parameters, effects of predicted response, and determination of parameters.

Table 2.2. Summary of SIMPLE DSS Input Parameters

Input Parameters	Effect of Predicted response	Determination of Prameters
β	Controls the sensitivity of the materials	Excess pore water pressure at large strains measured in a DSS test (γ=15-25%)
φ	Describe the Effective Stress Failure Envelope	Effective stress obliquity angle at large strains
m	Controls the undrained shear strength of the material	Determination from measured values of undrained strength, s_u (γ=15-25%)
G_n	Controls the small strain elastic shear modulus	Shear wave measurements (i.e., G_{max})
G_p	Controls the stress-strain during first loading from NC state	Calibration with measured stress-strain behavior.
θ	Controls the effective stress path for cyclic loading	Calibration with measured pore pressure development during cyclic loading

CHAPTR III

EXPERIMENTAL INVESTIGATION

3.1 INTRODUCTION

The main objective of work was to characterize the response of normally consolidated to lightly overconsolidated clays in submerged slope including experimental testing, constitutive modeling, and global analysis.

Twenty undrained direct simple shear tests, 8 monotonic and 12 cyclic, were performed on San Francisco Bay Mud known as Young Bay Mud at the University of California at Berkeley, using the U.C. Berkeley simple shear device. The detailed information about that apparatus was summarized by Biscontin (2001) in appendix B.2 of her dissertation. The clay samples were collected from the site of Hamilton Air Force Base using a fixed-piston, hand-pushed sampler attached to a 5 in diameter, thin-walled sampling tube. Table 3.1 gives the data for the index properties of Young Bay Mud under previous study based on the site of Hamilton Air Force Base. Young Bay Mud is a highly compressible soil with low shear strength and moderate sensitivity.

Table 3.1. Engineering Properties of YBM.

Reference	Liquid Limit (%)	Plastic Index (%)	In-situ W/C (%)	Unit weigth (kN/m3)
Duncan (1965)	88	45	88	14.6-15.1
Denby (1978)		34-51	52-99	13.5-15.6
Idriss et al. (1978)	81	49	89-95	14.5-14.6
Biscontin (2001)	99	59	89-99	14.3

3.2 TESTING REVIEW OF WORK OF BISCONTIN

3.2.1 Consolidation

The purpose of consolidations is to minimize the effects of sampling disturbance and obtain the normally consolidated specimen. Two types of consolidation procedure were performed, one consolidating under K_0 (CK_0) condition and the other consolidating under anisotropic (CK_α) condition to the same vertical effective stress, but under a shear stress. In the simple shear device, a sample is placed in a reinforced rubber membrane to prevent radial deformations and allow the sample to consolidate with or without applied shear stresses. The table 3.2 shows the consolidation information about all tests performed for her study.

3.2.2 Anisotropy

Casagrande and Carrillo (1944) defined the two components of anisotropy, inherent and induced anisotropy. Inherent anisotropy is defined as a physical characteristic of clay and independent of applied stresses. However, induced anisotropy is defined as a physical characteristic caused by the strain associated with the applied stresses and strains. Ladd (1991) also discussed anisotropy as related to an inherent and an initial component. The first component is caused by the initial one-dimensional deposition and K_0-consolidation, and the second component exists prior to the application of stresses. The proposed two concepts for anisotropy are divided in separate terms due to the soil structure and applied stresses (Yue, 2001). Because of the difficulty of measuring anisotropy many engineers are usually interested in the combined effects of anisotropy.

Table 3.2. Summary of Consolidation for Simple Shear Test on Young Bay Mud (Biscontin, 2001)

Consolidation	Test	Vertical Stress(kPa) (σ'_{vc})	End of Consolidation Stress Ratio (kPa)		End of Consolidation Strain (%)	
			τ_x/σ'_{vc}	τ_y/σ'_{vc}	γ_x	γ_y
CK_0	**BM-1**	67.10	-	-	0.140	0.140
	BM-2	88.60	-	-	0.000	0.341
	BM-3	87.60	-	-	-0.014	0.365
	BM-4	90.30	-	-	-0.011	0.620
	BM-5	86.90	-	-	-0.012	0.414
	BM-6	88.80	-	-	0.013	0.400
	BM-7	88.40	-	-	0.012	0.464
	BM-8	88.60	-	-	0.013	0.939
	BM-9	92.96	-	-	0.012	0.558
CK_α	**BM-11**	91.80	0.218	-0.040	18.074	0.426
	BM-12	93.00	0.233	-0.045	17.166	0.400
	BM-13	92.80	0.230	-0.045	16.531	0.419
	BM-15	93.30	-0.123	-0.144	-5.977	-6.997
	BM-16	91.46	0.201	-0.015	15.771	0.350
	BM-17	93.40	0.154	0.130	12.166	12.039
	BM-18	97.20	0.009	0.177	0.128	18.316
	BM-19	92.10	0.013	0.191	0.242	18.804
	BM-20	94.20	-0.002	0.189	0.356	17.441
	BM-21	93.19	0.004	0.190	0.170	19.342
	BM-22	93.20	-0.204	-0.002	-19.670	0.483
	BM-23	95.80	0.202	0.006	14.847	0.267

3.3 TEST RESULTS ON YOUNG BAY MUD

In the case of the eight K_0 consolidated tests with pore pressure measurements (CK_0U), only two samples were sheared monotonically in the X-direction to represent the ground level condition. One sample was sheared at the strain rate of 5%/hr and another was sheared at the strain rate of 50%/hr. Four samples were sheared in simple shear tests subjected to uniform cycles of shear loading with the amplitude of $\tau_{cyc} / \sigma'_{vc}$ of 0.15, 0.175, 0.2, and 0.25 and conventional frequency (0.1 Hz). The two remaining samples were both tested at $\tau_{cyc} / \sigma'_{vc}$ =0.1, however, the frequency was of 0.1Hz in one case and 1Hz in the other.

Anisotropically consolidated undrained shear tests ($CK_{\alpha}U$) were divided into three groups. The first group comprised multidirectional tests at several angles. The second group was cyclic tests with consolidation to a shear stress ratio of 0.2 with uniform cycles of shearing at $\tau_{cyc} / \sigma'_{vc}$ = 0.15, 0.175, 0.2. The third group was consolidated in the y-direction with the same shear stress ratio and uniform cycles of shear stress. Table 3.3 summarized the experiments. The direct simple shear apparatus was developed for testing samples of soils under conditions of simple shear (Fig. 3.1). In general, stress states in soil can be described by six independent normal and shear stress components in three dimensions. Engineers often assume a state of plane stress on the soil elements to simplify calculations. As a results, only two normal stresses (σ_x, σ_y) and a shear stress ($\tau_{xy,}$) component act on the soil elements. Similar to stress, the general state of strain is characterized by six components: three normal strain components (ε_x, ε_y, ε_z) and three shear strain components (γ_{xy}, γ_{xz}, γ_{yz}). If strain in one direction are zero (ε_z= γ_{xz}= γ_{yz}=0) then it is to assume a state of plane strain. A cylindrical soil sample is placed within a reinforced rubber membrane. This membrane enforces the zero extension (ε_x=0) during loading. Therefore, only one normal strain (ε_y) and one shear strain (γ_{xy}) remains. In the case of undrained condition, a constant volume test, there is no change in vertical displacement (ε_y=0). Finally, one shear strain component (γ_{xy}) is measured in simple shear test.

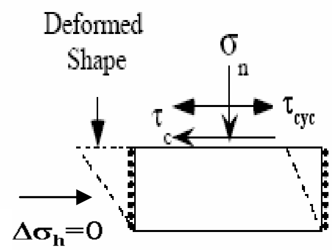

Fig. 3.1. Direct Simple Shear Stress Conditions

Table 3.3. Summary of Simple Shear Tests on Young Bay Mud (Biscontin, 2001).

Consolidation	Test	Consolidation Shear Stress (τ_c/σ'_p)	Angle δ(°)	Cyclic Shear Stress (τ_{cyc}/σ'_p)	Strain-Rate (%/hr)	Frequency (Hz)
CK_0	**BM-1**	0.00	0	0.1	-	1
	BM-2	0.00	0	monotonic	5	-
	BM-3	0.00	0	0.1	-	0.1
	BM-4	0.00	0	0.2	-	0.1
	BM-5	0.00	0	0.15	-	0.1
	BM-6	0.00	0	0.175	-	0.1
	BM-7	0.00	0	0.175	-	0.1
	BM-8	0.00	0	0.25	-	0.1
	BM-9	0.00	0	monotonic	50	-
CK_α	**BM-11**	0.20	180	monotonic	5	-
	BM-12	0.20	0	0.175	-	0.1
	BM-13	0.20	0	0.15	-	0.1
	BM-15	0.20	135	monotonic	5	-
	BM-16	0.20	0	0.2	-	0.1
	BM-17	0.20	45	monotonic	5	-
	BM-18	0.20	90	monotonic	5	-
	BM-19	0.20	90	0.175	-	0.1
	BM-20	0.20	90	0.2	-	0.1
	BM-21	0.20	90	0.25	-	0.1
	BM-22	0.20	180	monotonic	5	-
	BM-23	0.20	0	monotonic	5	-

3.3.1 Monotonic Tests

This section presents the soil response in the investigation of the initial consolidation shear stress and shear strain rate, with no consideration of the effect of the direction of the consolidation shear stress.

The undrained shear strength is influenced by the initial consolidation shear stress and shear strain rate. In order to clarify the influence of an initial shear stress and strain rate on the response of the soil, monotonic tests were performed. Biscontin notes in discussing her experimental results in monotonic shearing that “All tests reach approximately the same condition in the stress path space, for a stress ratio $\tau/\sigma'_v=\psi$ of 25° and a normalized peak shear stress at large strains (15~20%) of 0.27.” Rau (1999) studied the soil response in simple shear with the same soil (YBM). The results of monotonic tests on normally consolidated samples are presented in Table 3.4 and Fig 3.2 Rau (1999) concluded that the undrained shear strength ratio ranging from 0.22 to 0.3 at 7.5% shear strain failure. The undrained shear strength is defined by the maximum normalized shear stress level for simple shear tests. This strain at failure is lower than the strains reached by Biscontin’s tests.

Table 3.4. Monotonic Testing Results for NC Clay (Rau, 1999)

Test No.	Vertical Effective Consolidation Stress, σ'_{vc} (kPa)	Shear Strain at Failure (%)	Shear Stress at Failure, τ_f (kPa)	Undrained Strength Ratio, τ_f/σ'_{vc}
Mono-1	68	7.5	20	0.3
Mono-2	67	7.5	19	0.29
Mono-3	254	7.5	56	0.22
Mono-4	160	7.5	41	0.26
Mono-8	119	7.5	30	0.25

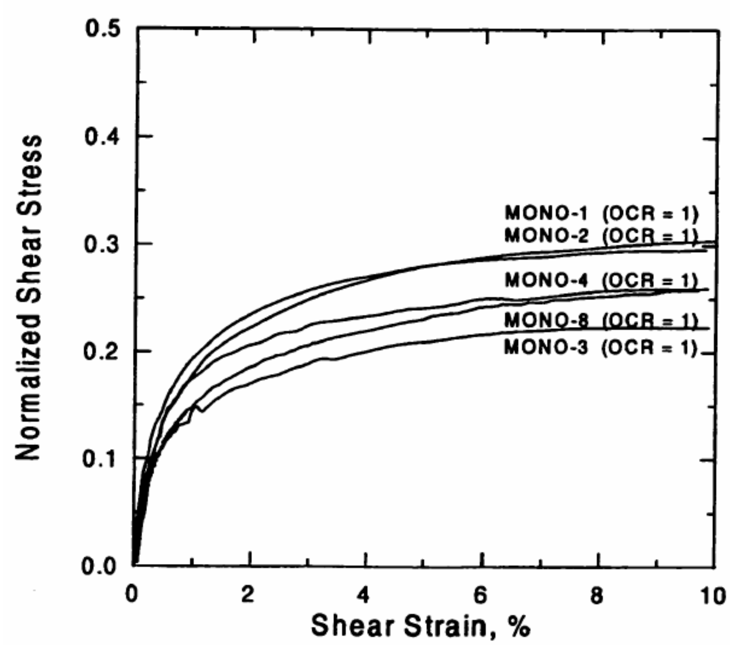

Fig 3.2. Stress-Strain Curves for Monotonic Tests on NC YBM (after Rau, 1999)

If a consolidation shear stress is applied to samples, higher undrained shear strength is reached (Fig 3.3). Test BM-2 was sheared under the standard rate of strain (5%/hr) with consolidation stress ratio equal to zero. Test BM-23 was consolidated to a normalized shear stress of 0.2, and then sheared in the same direction with the standard strain rate. The results show a moderate increase in shear stress at the beginning and a continuous increase in shear stress up to peak shear stress.

At large strain conditions, BM-2 and BM-23 have an undrained shear strength value of 0.27 and 0.33 respectively. For normally consolidated clay, higher initial shear stress results in a decrease in pore pressure generation during shearing, while the failure envelope remains the same.

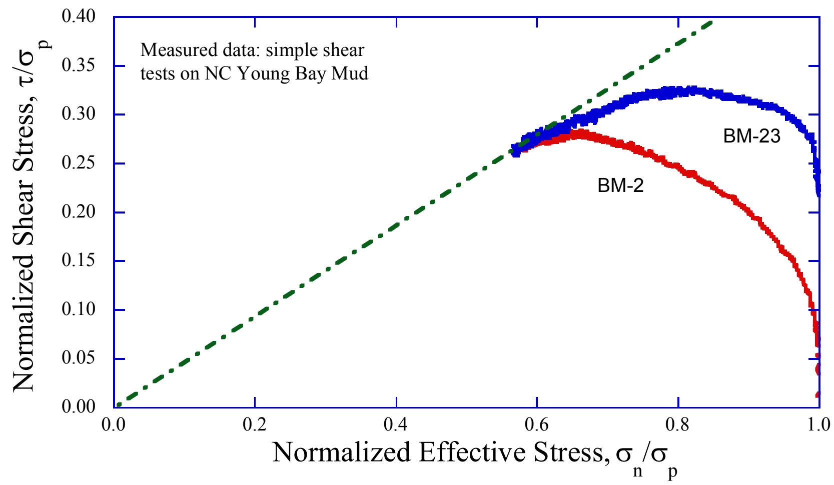

(a) Stress Path

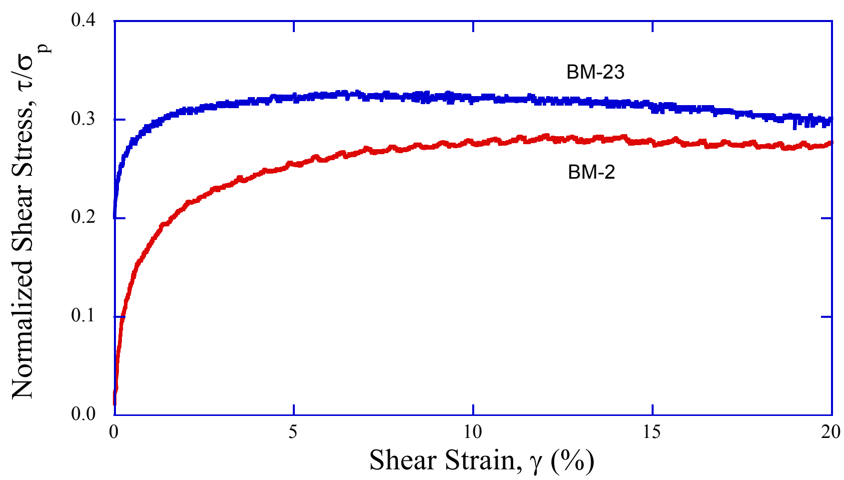

(b) Stress-Strain Curve

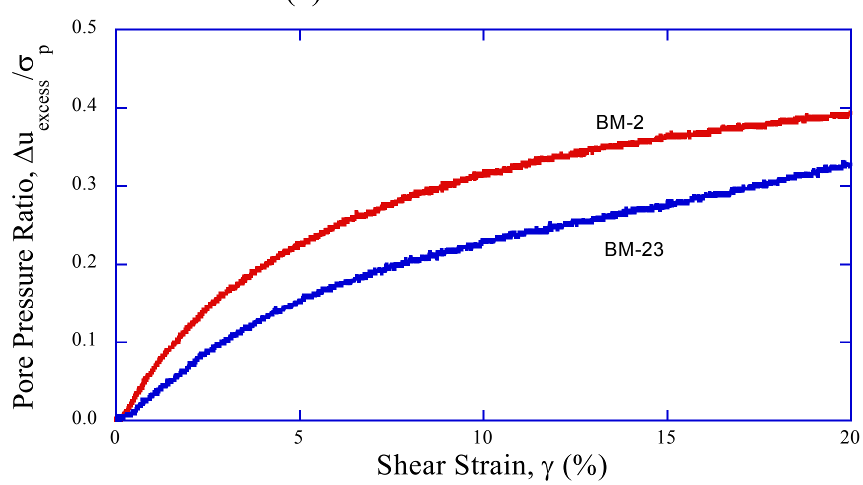

(c) Pore Pressure Generation

Fig. 3.3. Test Results of BM-2 and BM-23 (Effect of Consolidation Stress History)

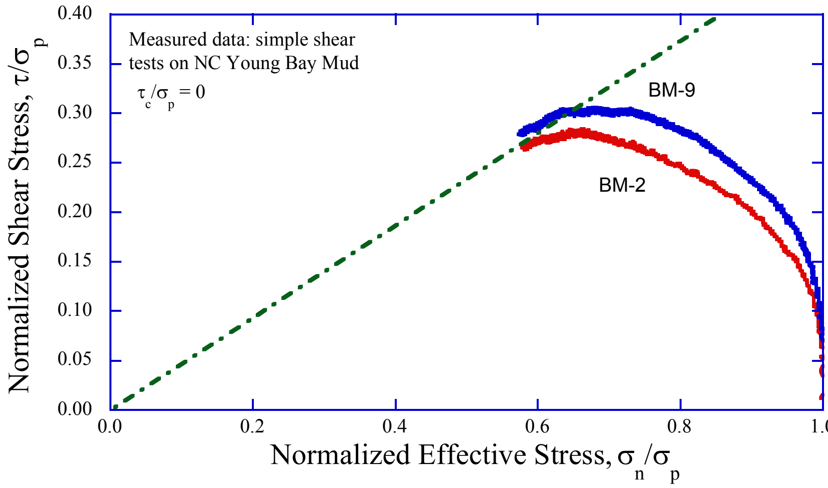

(a) Stress Path

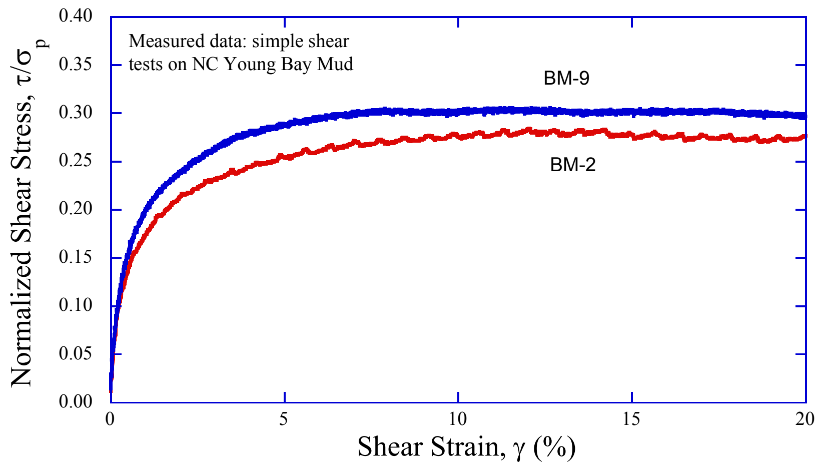

(b) Stress-Strain Curve

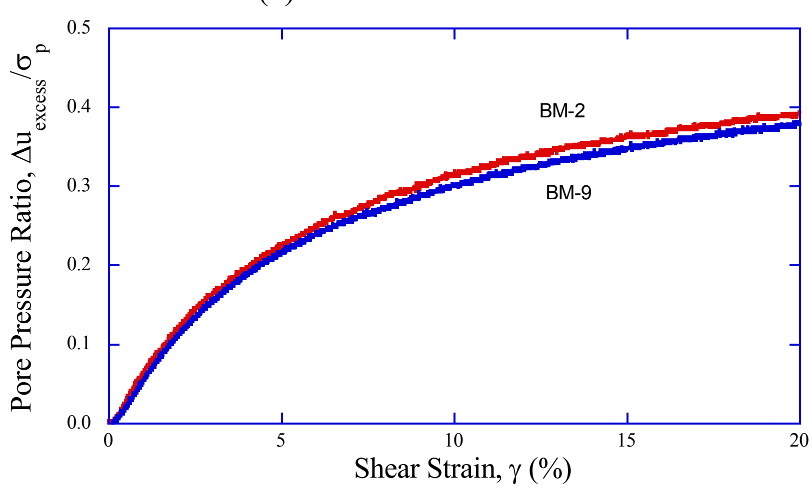

(c) Pore Pressure Generation

Fig. 3.4. Test Results of BM-2 and BM-9 (Effect of Strain Rate)

Among monotonic simple shear tests, only two different strain rates were performed by 5 and 50%/hr both with τ_c / σ'_{vc} =0. The results of the two experiments show in Fig 3.4 that the undrained shear strength depends on shear strain rate. A sample sheared at 50%/hr reaches the maximum undrained shear strength of 0.3 comparing 0.27 of sample sheared at 5%/hr. the undrained shear strength value obtained on between 5% and 50%/hr is about 11% for a change in a tenfold strain rate. The stress-strain response also shows a stiffer behavior for a higher strain rate. For normally consolidated clay, higher strain rate results in a decrease in pore pressure generation during shearing, while the shear strength envelope is slightly different.

3.3.2 Cyclic Tests

For samples subjected to undrained shear loading, the cyclic shearing behavior depends upon two main factors: the build up of pore water pressure leading to a reduction in normal effective stress and the accumulation of shear strain.

The first group of six samples in CK_0U tests was sheared in simple shear tests subjected to uniform cycles of shear loading with the amplitude of $\tau_{cyc} / \sigma'_{vc}$ of 0.15, 0.175, 0.2, and 0.25 and conventional frequency (0.1 Hz) after K_0 consolidation. In the cyclic tests, both development of excess pore pressure and accumulation of plastic strains with increasing number of cycles were typically observed. Fig. 3.5 shows the normalized shear strength and pore pressure generation with log of number of cycles at different cyclic stress ratios. The development of pore pressure was steadily increasing.

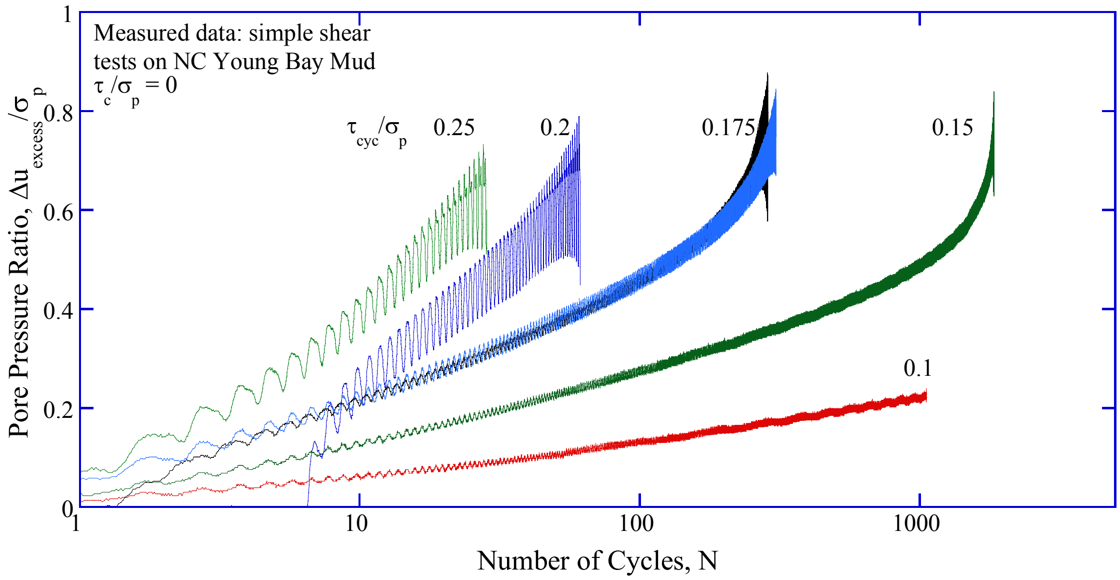

(a) Development of Pore Pressure

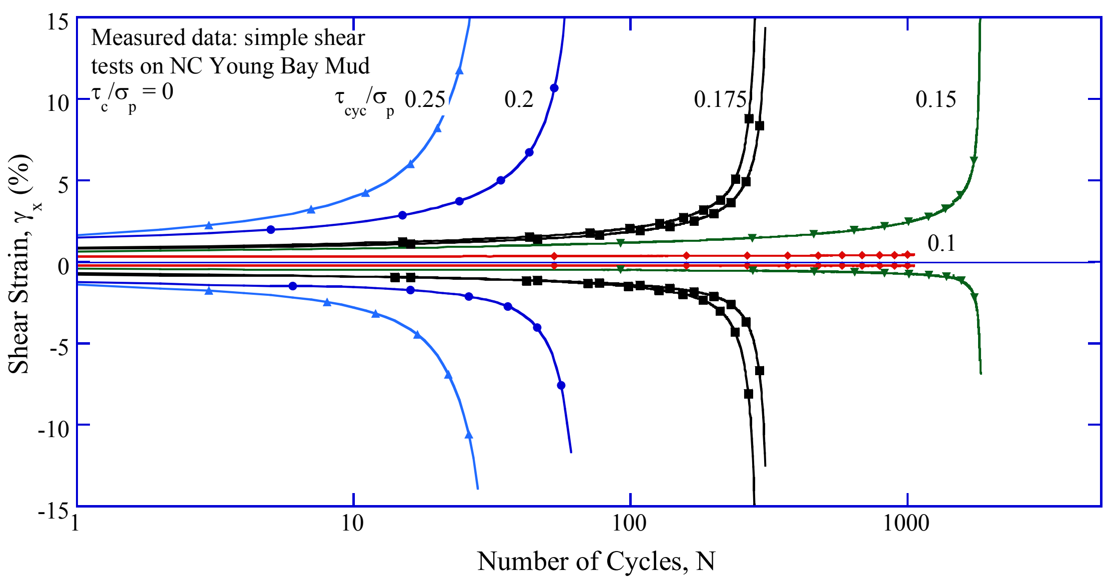

(b) Accumulation of Plastic Strains

Fig. 3.5. Results of Cyclic Test in CK_0U Tests

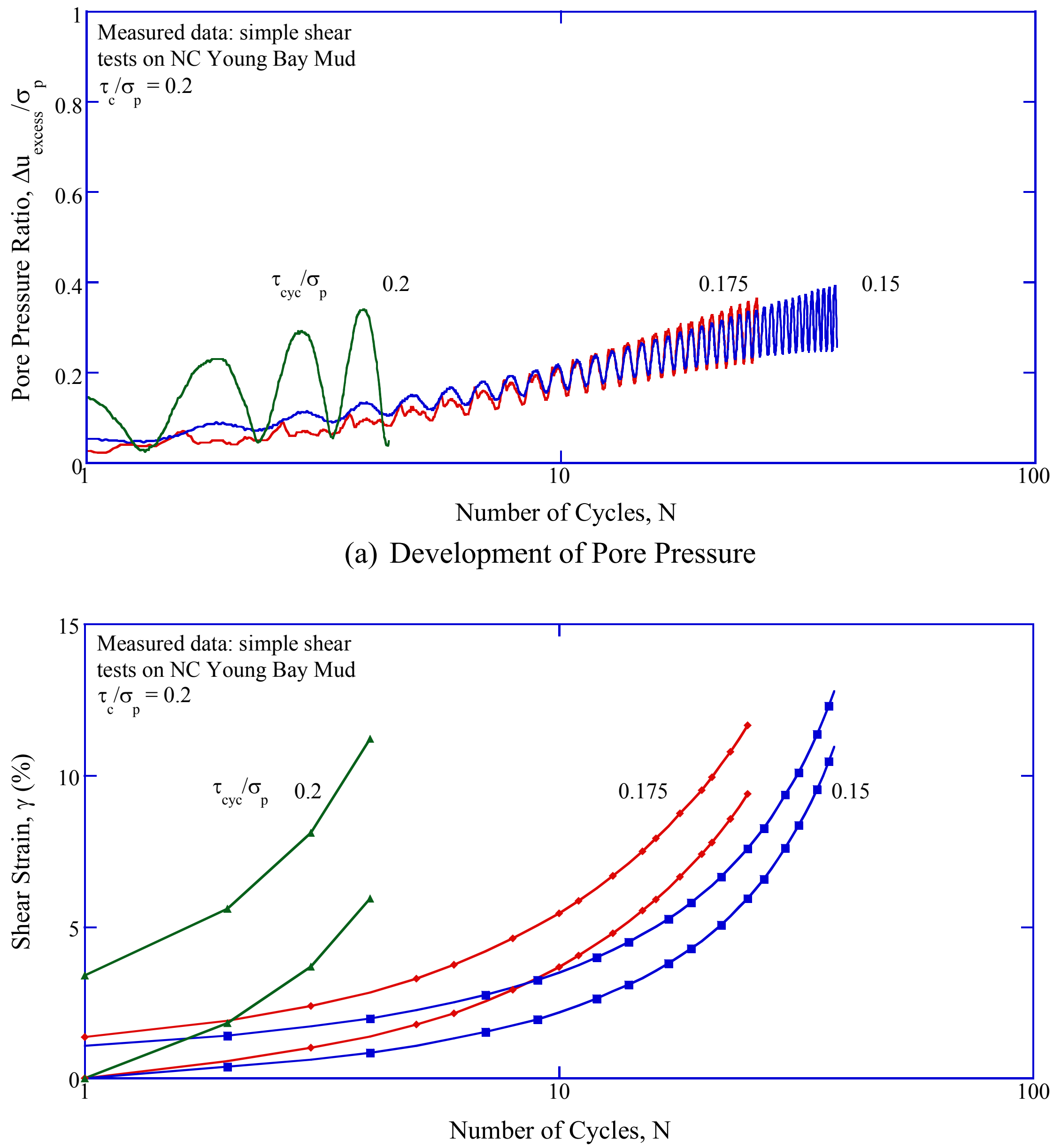

(a) Development of Pore Pressure

(b) Accumulation of Plastic Strains

Fig. 3.6. Results of Cyclic Test in $CK_{\alpha}U$ Tests

At failure, the pore pressure stabilizes at its maximum value. The shear strain versus number of cycles showed a maximum and minimum value of shear strain to each cycle and mostly symmetric response. The curve of pore pressure and shear strain versus number of cycle was very smooth, especially for test BM-3 (τ_{cyc}/σ'_{vc}=0.1) which did not fail even after a large number of cycle. The strains and excess pore pressures at the first loading cycle increase with increase in cyclic stress ratio (CSR).

The second group of cyclic tests was also consolidated to a shear stress ratio of 0.2, then sheared with uniform cycles of shear stress, τ_{cyc}/σ'_{vc} = 0.15, 0.175, 0.20 in the same direction as the first group and 1Hz frequency to define the effect of anisotropy. Fig. 3.6 shows the normalized shear strength and pore pressure generation with log of number of cycles at different cyclic stress ratios. The curve of pore pressure and shear strain versus number of cycles, especially BM-16 (τ_{cyc}/σ'_{vc}=0.2) showed failure in very few cycles. There are big differences between isotropic and anisotropic conditions. In the case of anisotropic conditions, negative shear strains were not induced by loading. The average shear strain increases with increase in the number of cycles. The effects of initial shear stress indicate that the accumulation of shear strains reach 10% shear strains at the lower number of cycles compared to the CK_0U. Similarly, the excess pore pressure generation at failure is reached fairly rapidly with a lower number of cycles when there is an initial static shear stress.

In some of the cyclic test, the samples failed within a few cycles. For both monotonic and cyclic tests, the undrained shear strength has a dependence on strain rate.

Table 3.5, Fig 3.7, and Fig 3.8 indicate the strain rate in the first cycle corresponding to loading at different cyclic shear stress ratio. The strain in the first cycle increases with the amplitude of the cyclic stress resulting in a higher strain rate. Because the frequency was 0.1Hz, the period was 10 seconds, the shear strains developed in 2.5 seconds. The shear strain at 0.25 cycle, first loading part, obtained in cyclic tests range roughly between 400 and 2000%/hr, and 1300 and 4000%/hr for CK_0U and $CK_\alpha U$ respectively, while samples were sheared at 5%/hr for monotonic tests. These results show that the strain rate in cyclic tests is about 80 to 800 times the strain rate in monotonic tests.

Lefebvre and LeBoeuf (1987) also observed that in the cyclic loading the strain rate is much higher comparing the strain rate in usual monotonic tests. In these tests, the effects of strain rate in cyclic response at the first cycle in direct simple shear are confirmed. Therefore, the strain rate effects are more significant for cyclic tests in simple shear.

Table 3.5. Strain Rate with the Amplitude of Cyclic Shear Stress Ratio at the First Cycle

Consolidation	Test	Consolidation Shear Stress (τ_c/σ_p)	Cyclic Shear Stress Ratio (τ_{cyc}/σ_p)	Strain Rate (%/hour)
CK_0U	BM-3	0.00	0.100	389
	BM-4	0.00	0.200	1930
	BM-5	0.00	0.150	864
	BM-6	0.00	0.175	1166
	BM-7	0.00	0.175	1166
	BM-8	0.00	0.250	2045
$CK_\alpha U$	BM-12	0.20	0.175	1660
	BM-13	0.20	0.150	1304
	BM-16	0.20	0.200	3725

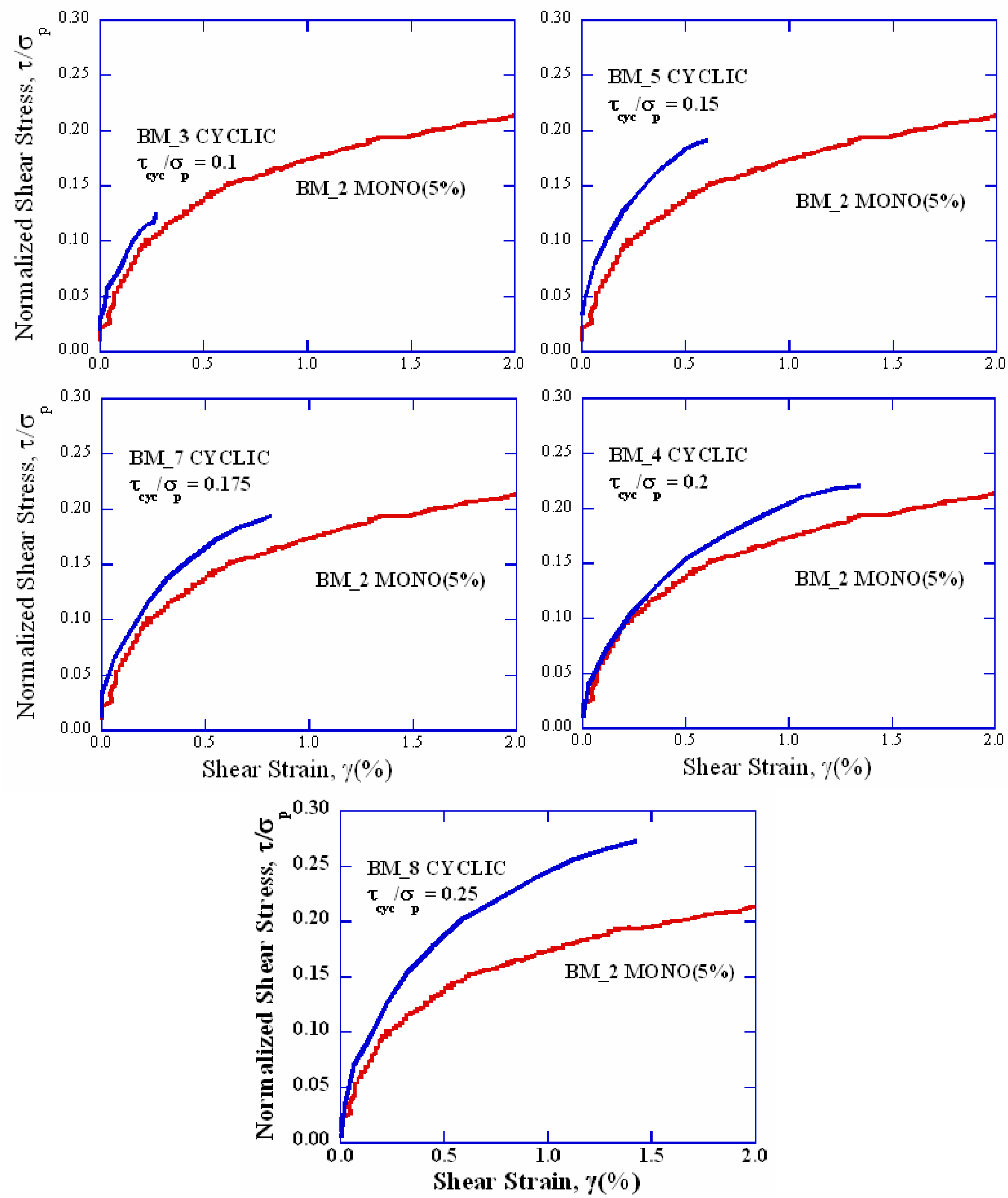

Fig. 3.7. Stress-Strain Relationship in First Loading Cycle (τ_c / σ'_{vc} =0)

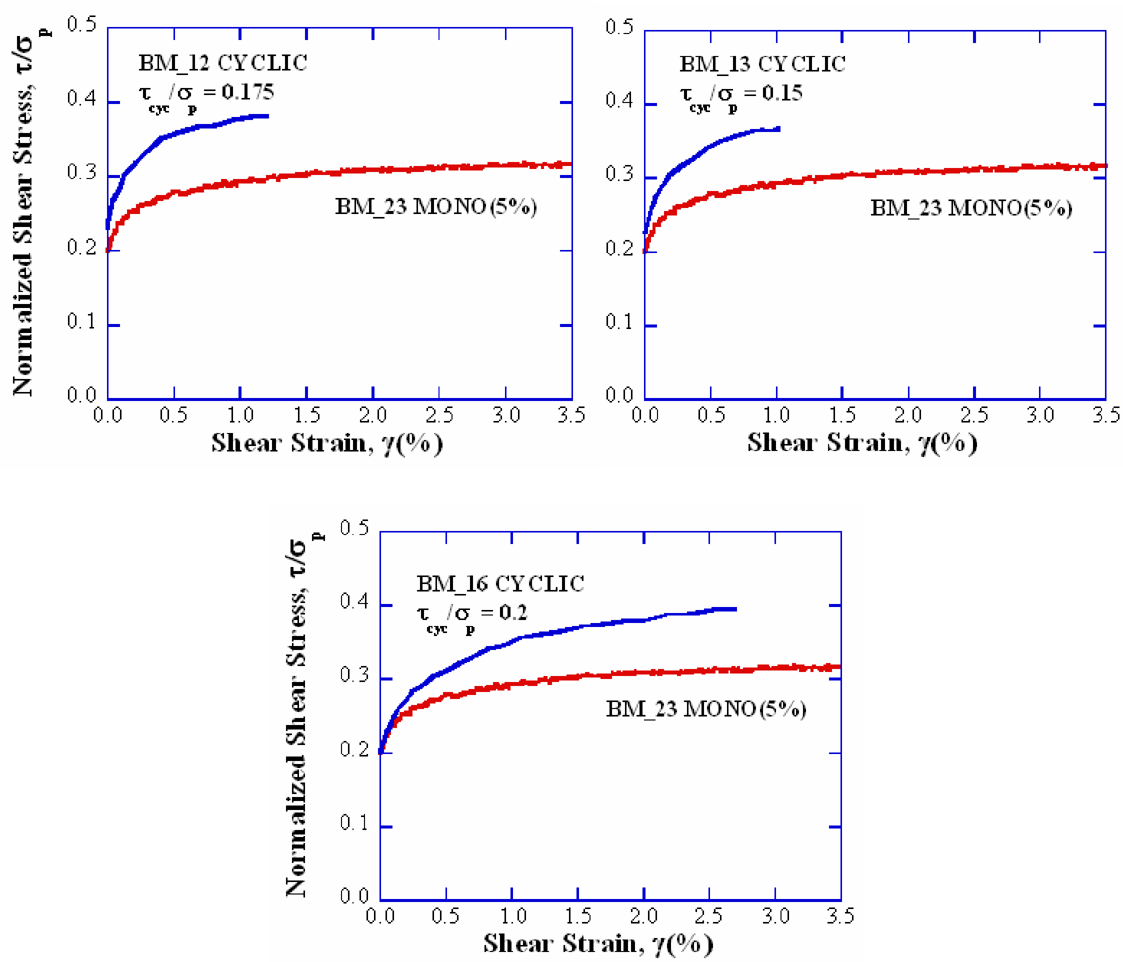

Fig. 3.8. Stress-Strain Relationship in First Loading Cycle ($\tau_c / \sigma'_{vc} = 0.2$)

3.4 CONCLUSIONS

A series of simple tests were conducted on YBM samples for both monotonic and cyclic tests to investigate the effect of a consolidation shear stress. The results for undrained direct simple shear tests on YBM clearly indicate the importance of soil response in monotonic response including the effect of initial consolidation stress and strain rate. Although the importance of the strain rate effect on soil response, only two monotonic tests at different rates could not purport to be a full study for the effect of strain rate on Young Bay Mud in simple shear, but they can present at least an initial assessment of the problem (Biscontin, 2001). The monotonic tests showed that the maximum shear stress depends on both the initial shear stress and the rate of strain of undrained shearing. As initial shear stress and strain rate increase the undrained shear strength also increase, but pore pressure decrease.

From cyclic tests, following observations are generally deduced:

- the excess pore pressure generation increasing with increase in cyclic stress ratio (CSR);

- faster rate of excess pore pressure accumulation in the first few cycles with increase in cyclic stress ratio (CSR);

- increasing with the amplitude of the cyclic stress resulting the higher strain rate.

There are large differences in shear strain behavior with number of cycles between CK_0U and $CK_\alpha U$ cyclic tests. In the case of the tests with no consolidation shear stress, the shear strains are symmetrical and the average shear strains are around zero strain. The tested responses with an initial shear stress present a much different behavior. The average shear strain increases with the number of cycles. In Fig 3.7 and 3.8, the cyclic strain curves at the first cycle are above the monotonic curve. Therefore, the strain rate in cyclic response is much higher than those of monotonic tests.

3.5 DISCUSSION

The importance of effects of strain rate in behavior of cohesive soil has long been investigated by many researchers (Housel 1960; Perloff 1962; Lefebvre and LeBoeuf 1987; Awoleye et al. 1991; Katti et al. 2003). The early investigations on clay focus on the general recognition of the increased shear strength of clay soils under faster rates of loading. Then, they suggested additional work on rate effects is necessary to determine the static resistance including the measurements for several rates of deformation. In the middle of the twentieth century, the literature and experimental reviews mentioned that the undrained shear strength is highly influenced by strain rate, both in monotonic and cyclic test. Nevertheless, the few results are limited in terms of the conditions explored in the various experimental works and a reasonable formulation is questionable. The literature reviews established the fact that the soil responses show a unique relationship between shear strength and log scale of strain rate. Graham et al. (1983) proposed a strain-rate parameter, $\rho_{0.1}$, expressed as a percentage of the shear strength measured at 0.1%/hr of strain rate to represent the change in shear strength with strain rate. Furthermore, Sheahan et al. (1996) similarly defined a more general strain-rate parameter as mentioned in the literature review. This strain-rate parameter is a useful concept and helps in predicting reliable results for investigating the undrained shear strength of clay soils under varying conditions of strain rates. Lefebvre and LeBoeuf (1987) study confirms that the strain rate effect on undrained shear strength appears to be the same for both normally consolidated and slightly over consolidated soil. In the typical shear test, samples were sheared at the lower strain rate comparing the dynamic loading, such as vibration and earthquake. The testing model defined by Andersen (1991) indicates that shear strength of soils under dynamic loading are very complex. Therefore, trixial compression, extension, and direct simple shear tests should be performed in the laboratory test program. Several researchers have performed simple shear test with Boston Blue Clay (Malek, 1987; DeGroot, 1989) to investigate the effect of consolidation history on monotonic and cyclic tests, and multidirectional loading. Konard and Wagg (1993) indicated that monotonic and cyclic tests describe the same strength envelope at the same strain rate. In spite of the importance of time dependency on the stress-strain-strength response of clays there are only few tests addressing this issue, especially in simple shear. Based on reviews, modeling of soils is necessary to describe the effect of strain rate. Biscontin (2001) raised a question concerning the relative importance of strain rate on clay in simple shear but available data were very limited. Biscontin's SIMPLE DSS model described the effects of initial shear stress and multidirectional loading for both monotonic and cyclic tests. To describe the soil response, the SIMPLE DSS model requires the seven parameters as mentioned in chapter II. The parametric study gives an idea that if data from experimental tests are established to account for the effect of strain rate on shear strength, then a unique relation can be obtained. Among these input parameters, this research focuses on one parameter known as slenderness parameter, m, which primarily controls the undrained shear strength to include the strain rate effect in the new model.

The literature reviews cover almost all the aspects of monotonic and cyclic response on cohesive soils. Experimental and modeling investigations have established the importance of several effects regarding shear stress, consolidation history, and strain rate. The study indicates how to use each part of SIMPLE DSS model to define the shear strength after the application of strain rate effects.

CHAPTER IV

MODELING OF MODIFIED SIMPLE DSS

4.1 INTRODUCTION

In soil mechanics, the stress-strain-strength relationship of saturated clays is affected by loading condition, and has been studied by many researchers. The important role of shear strength, τ, has been considered for many years, and generalized the constitutive models based on critical state and bounding surface condition is established well on triaxial, vane shear, pressure meter, and direct simple shear tests.

However, the rate of strain effects has been considered by only few researchers in direct simple shear test. The direct simple shear test device was developed for testing soil samples under conditions of simple shear and plane strain. Generally, the samples in direct simple shear (DSS) test were consolidated under given effective normal stress, σ_n, and applied shear stress, τ . After the consolidation, the samples were sheared monotonically and cyclic.

This chapter presents a modified simple effective stress model, referred to as the modified SIMPLE DSS model; to describe the monotonic and cyclic response with effect of strain rate for normally consolidated cohesive soils in direct simple shear. The SIMPLE DSS model was reviewed already in literature review. The propose model is developed from original SIMPLE DSS model related with the framework of bounding surface. Hence, only equations relevant to SIMPLE DSS are recalled and addressed in this chapter.

4.2 TYPICAL TRENDS OF CYCLIC DSS TEST

4.2.1 Stress Controlled Test

Fig. 4.1 shows the typical time history of shear stress applied in a stress-controlled DSS test. The major features indicated:

(1) as the number of cycle increases the cyclic strain increase, eventually becoming a significant increase.

(2) as the number of cycle increases the pore water pressure continuous increase.

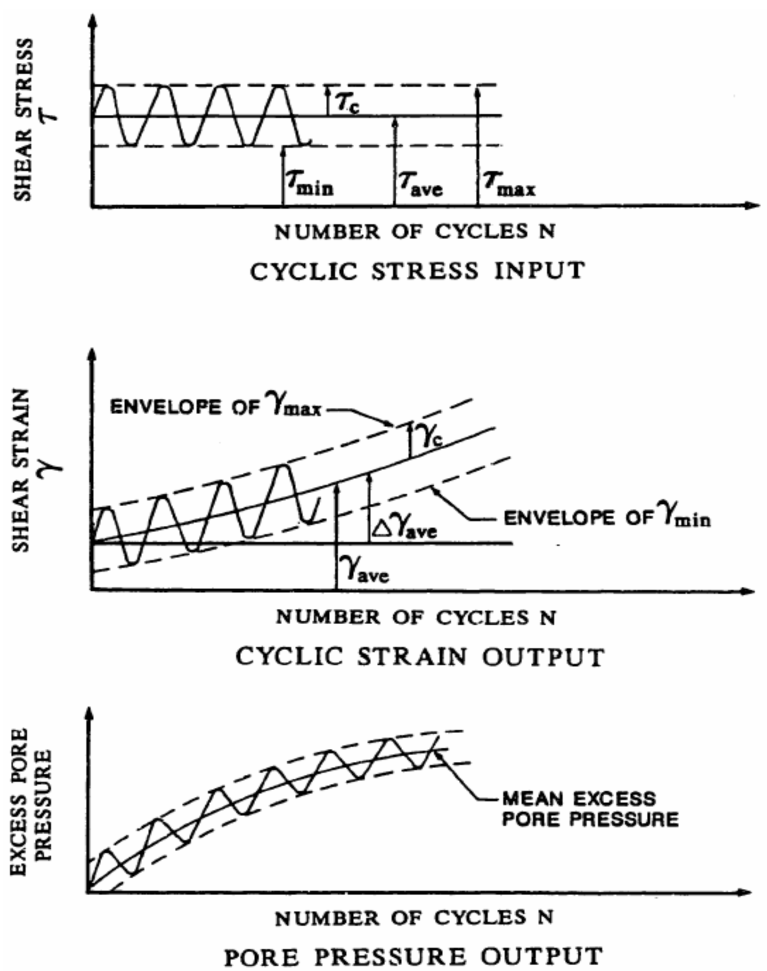

Fig. 4.1. Stress Controlled Test (Malek, 1987)

4.2.2 Strain Controlled Test

Fig. 4.2 shows the typical time history of shear stress applied in a stress-controlled DSS test. The major features indicated:

(1) as the number of cycle increases the cyclic stress decrease.

(2) as the number of cycle increases the pore water pressure continuous increase.

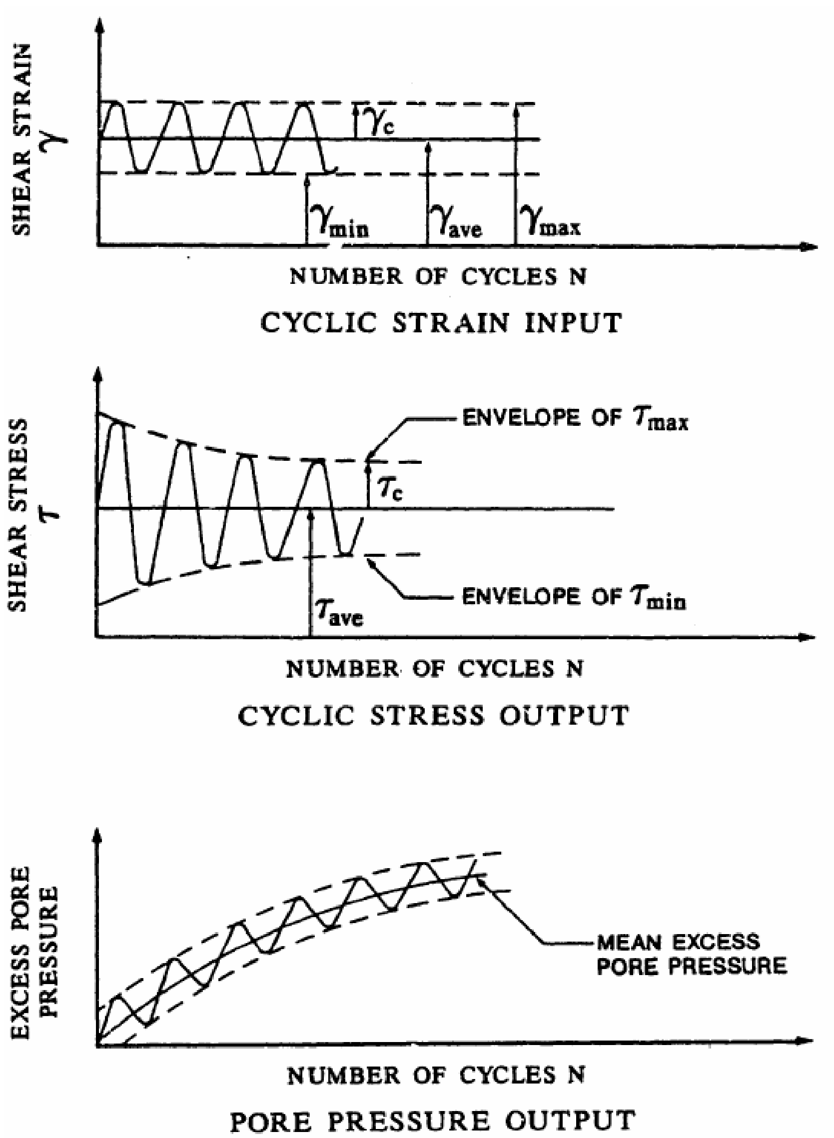

Fig. 4.2. Strain Controlled Test (Malek,1987)

4.3 MODELING OF SIMPLE DSS WITH STRAIN RATE

4.3.1 Assumptions

The normalized shear strength ratio was shown to have a linear relationship with the log scale of strain rate have a linear relationship (Lefebvre and LeBoeuf 1987; Murakami et al. 1996: Awoleye et al. 1991; Zhu and Yin 2002; Katti et al. 2003). To include the effects of strain rate, the modified simple effective stress model start with two assumption: (1) a specific shear strength corresponds to a specific strain rate in a unique relation; and (2) the effect of strain rate does not change the failure envelope (i.e. β and φ is const.).

The Eq. (4.1) is modified from Sheahan et al. (1996). The strength increase with strain can be described by a log-linear law, requiring three parameters.

$$s_u = s_{u0}\left(1+\rho_{\dot{\gamma}}\log\left(\frac{\dot{\gamma}}{\dot{\gamma}_0}\right)\right) \tag{4.1}$$

Where,

s_{u0} = reference strength at a specified reference strain rate ($\dot{\gamma}_0$).

$\rho_{\dot{\gamma}}$ = rate of increase in strength with change in strain rate.

$\dot{\gamma}$ = strain rate$\left(\dfrac{\Delta\gamma}{\Delta t}\right)$.

$\dot{\gamma}_0$ = reference strain rate.

The parameter, $\rho_{\dot{\gamma}}$, can be determined from laboratory experiments with different strain rates.

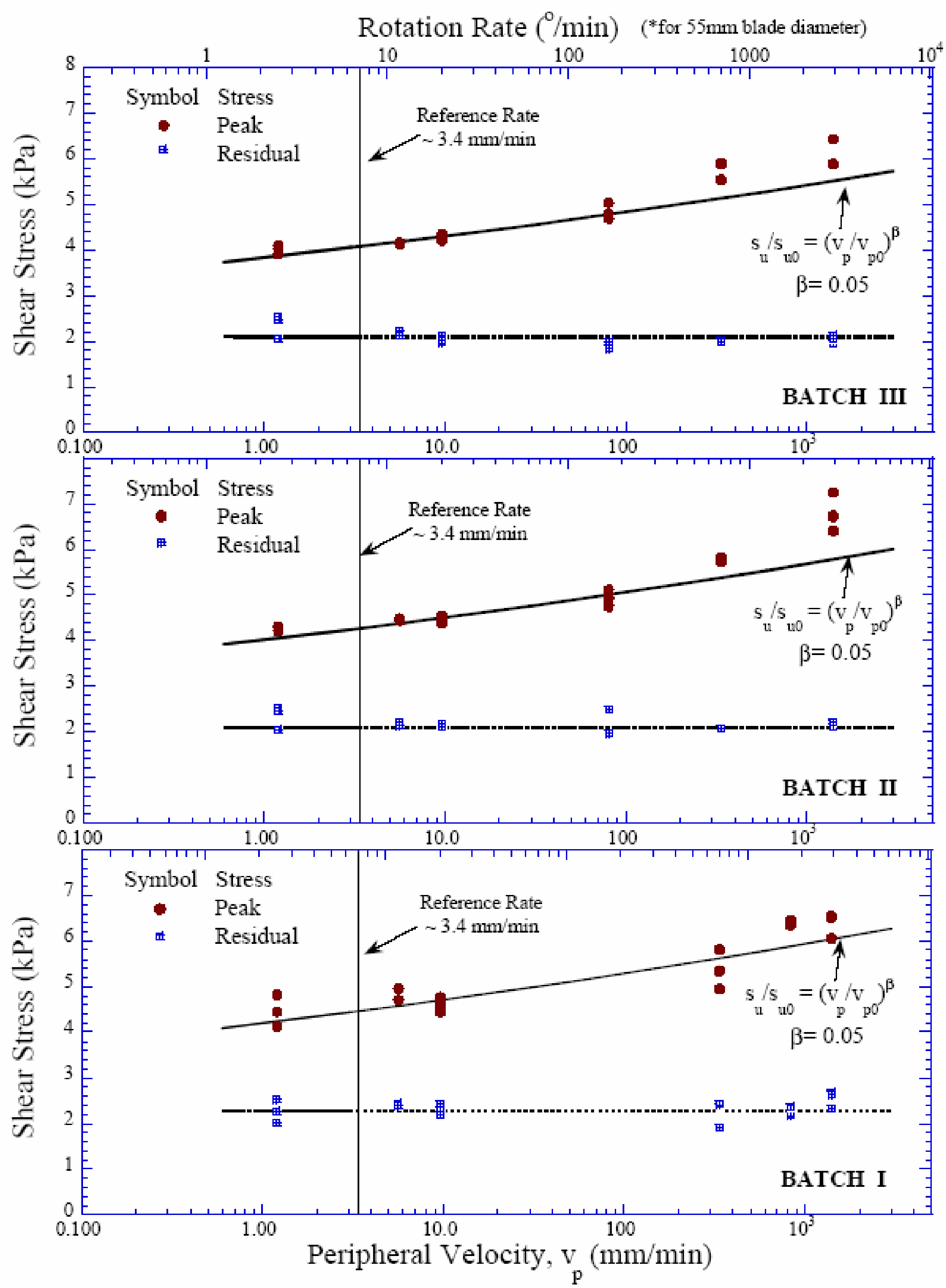

Fig. 4.3. Measured Peak and Undrained Residual Strength from Vane Test
(after Biscontin and Pestana, 1999)

Fig. 4.3 shows the measured peak and residual strength for three different batches of an artificial soil (Biscontin and Pestana, 1999). It is clear that the peak shear stress increases with increase in a peripheral velocity which can be taken as an indication of strain rate. In contrast, the residual strength shows an identical response with strain rate. The residual strength defined by the ultimate strength at large strain condition can not be affected by the peripheral velocity. This soil's response supports the assumption that the failure envelope is independent of strain rate in the same soil.

4.3.2 Monotonic Response

The effective stress path, pore pressure generation, during standard monotonic simple shear is described by following Eq. (4.2a). This equation is only available for no consolidation shear stress condition, referred to as the standard simple shear test ($\tau_c = 0$).

$$\eta^2 - \tan^2\varphi + \tan^2\varphi \left[\frac{\left(\dfrac{\sigma_n}{\sigma_p}\right)^m - \beta^m}{1-\beta^m} \right] = 0 \tag{4.2a}$$

The Eq. (4.2b) can be applied when consolidation shear stress ($\tau_c \neq 0$) is present.

$$\eta^2 - \tan^2\varphi + (\tan^2\varphi + 0.8\eta_c^2 - 1.8\eta_c\eta) \left[\frac{\left(\dfrac{\sigma_n}{\sigma_p}\right)^m - \beta^m}{1-\beta^m} \right] = 0 \tag{4.2b}$$

Where ,

$\eta = \dfrac{\tau}{\sigma_n}$ = the shear stress ratio in normal shear stress space.

$\eta_c = \dfrac{\tau_c}{\sigma_p}$ =the consolidation stress ratio representing a slope.

$\tan\varphi$ = the shear stress ratio at failure.

β = the material parameter defining the normalized effective stress at failure.

m = the material parameter defining the slenderness.

The peak shear stress for standard simple shear test can be calculated from Eq. (4.3) when $\dfrac{\partial\tau}{\partial\sigma_n} = 0$, as a function of the material parameters β, φ and m.

$$\frac{s_{uo}}{\sigma_p} = \tan\varphi\left(\frac{2}{2+m}\right)^{\frac{1}{m}}\left(\frac{1}{\left(\frac{2}{m}+1\right)\left(1-\beta^m\right)}\right)^{\frac{1}{2}} \tag{4.3}$$

Where,

s_{uo} = undrained shear strength for no consolidation shear stress ($\tau_c = 0$).

Therefore, a specific parameter, m, controlling strength will be automatically changed based on the predicted strength.

The normal effective stress under monotonic loading condition is defined as

$$\sigma_n = \sigma_p \left[\beta^m + (1-\beta^m)\left(\frac{\tan^2\varphi - \eta^2}{\tan^2\varphi + 0.8\eta_c^2 - 1.8\eta_c\eta} \right) \right]^{\frac{1}{m}} \tag{4.4}$$

This equation is generalized from the Eq. (4.1) and (4.2).

In monotonic stress-strain relationship, "the response is described in terms of the change of the stress ratio, η, as a function of changes in shear strain, $\Delta\gamma$ (Biscontin, 2001) ." The direct simple shear stiffness, $\frac{\partial\eta}{\partial\gamma}$, are decomposed additively into an elastic, $\left(\frac{\partial\eta}{\partial\gamma}\right)^e$, and a plastic, $\left(\frac{\partial\eta}{\partial\gamma}\right)^p$, component. That is,

$$\frac{\partial\eta}{\partial\gamma} = \left(\frac{1}{\left(\frac{\partial\eta}{\partial\gamma}\right)^e} + \frac{1}{\left(\frac{\partial\eta}{\partial\gamma}\right)^p} \right)^{-1} \tag{4.5}$$

The elastic component can be represented using following expression. That is,

$$\left(\frac{\partial\eta}{\partial\gamma}\right)^e = G_n \left(\frac{\sigma_p}{\sigma_n}\right)^{0.5} \text{ where } G_n = \frac{G_{\max}}{\sigma_p} \tag{4.6}$$

G_n is a material parameter controlling the relation between the small strain modulus ($G_{\max}$) for normally consolidated states and the value of maximum past pressure. Small strain modulus ($G_{\max}$) is usually determined from in-situ shear velocity profile or by lower strain range vibration test such as the resonant column test. The elastic component is related to effective stress increment. The plastic component can be described by following expression. That is,

$$\left(\frac{\partial\eta}{\partial\gamma}\right)^{p} = G_p \frac{\tan\varphi - sign(\eta_c,\Delta\gamma)\eta_c}{\eta-\eta_c}\left[\tan\varphi - sign(\eta,\Delta\gamma)\eta\right] \qquad \text{for } \tau_c \neq 0 \qquad (4.7)$$

Where, G_p is the material parameter representing the first loading for normally consolidated specimens.

The monotonic simple shear tests are usually conducted as a strain controlled test. Fig 4.4 shows the flow chart of the code developed using matlab based on the iterative procedure for monotonic response with strain control. Every step follows the SIMPLE DSS model, except the slenderness parameter, m, is updated for the changing strain rate during the iterations. In first part, the material parameters are set up, all parameters can be selected through a short parametric study. Parameter, m, at reference strain rate is base on the reference strength defined from Eq. (4.3). The undrained shear strength based on the Eq. (4.3) is a function of material parameter m only, because the material parameters β and ψ, are constant according to the initial assumptions. The specific undrained shear strength corresponding to specific strain rate is already assumed using Eq. (4.1). Therefore, the peak shear stresses calculated with Eq. (4.1) and (4.3) based on the specific strain rate must have the same strength level obtained by changing the value of the slenderness parameter.

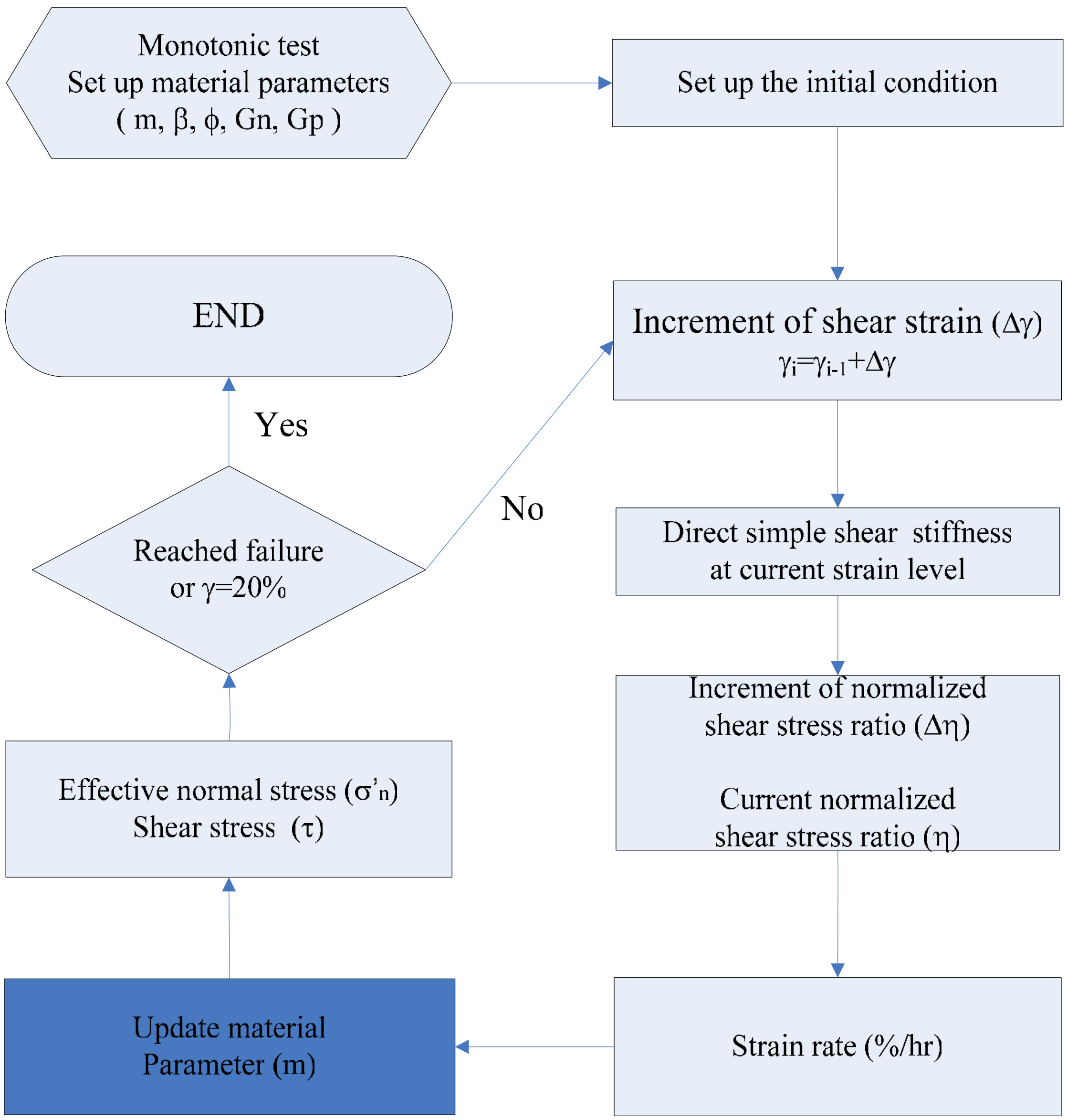

Fig. 4.4. Flow Chart of Modeling of Monotonic Response.

4.3.3. Cyclic Response

The shear strength under cyclic loading is influenced by the same factors which affect the strength of monotonic test: initial shear stresses, consolidation stresses, history of stress, and strain rate. Though cyclic strength has some of the same characteristics, cyclic loading has significantly different characteristics. In the case of cyclic loading induced by seismic forces, the strain rates are much higher than those in conventional monotonic loading (Lefebvre and LeBoeuf 1987) and even most laboratory cyclic loading. Obviously, failure does not occur in the first cycle at all. A similar approach to the monotonic test is used to model the cyclic test stress-controlled test. The pore pressure is generally increased with increasing number of cycles. The effective stress path (pore water pressure) is controlled by a load state surface during cyclic loading (Pestana et al. 2000).

The shape of transitional state is affected by the shear stress ratio, η_{rev}, θ and normal effective stress, σ_{nrev}, at previous reversal point. The current stress ratio can be calculated following Eq. (4.8).

$$\eta^2 - \frac{\tan^2\varphi}{1-\beta^m} - \left[\frac{\tan^2\varphi}{1-\beta^m} + \eta_{rev}^2 - 2\eta_{rev}\eta\right]\left(\frac{\sigma_n}{\sigma_{nrev}}\right)^{\frac{1}{B}} = 0 \qquad (4.8)$$

$$B = \frac{1}{\theta}\left(\frac{\sigma_{nrev}}{\sigma_p}\right)^2$$

Where,

η = current stress ratio.

η_{rev} = stress ratio corresponding to the last reversal point.

σ_{nrev} = normal effective stress corresponding to the last reversal point.

θ = strain rate dependent material parameter.

If the plastic surface is activated, then shearing will continue in the same loading direction. This shearing produces an increase with effective normal and shear stresses, and a decrease with excess pore pressure and stress ratio. The normal effective stress can be constructed as following:

-On plastic surface

$$\sigma_n = \sigma_p \left[\beta^m + (1-\beta^m)\left(\frac{\tan^2\varphi - \eta^2}{\tan^2\varphi + 0.8\eta_{rev}^2 - 1.8\eta_{rev}\eta} \right) \right]^{\frac{1}{m}} \tag{4.9.a}$$

-Inside of plastic surface

$$\sigma_n = \sigma_{nrev} \left[\frac{\tan^2\varphi - \eta^2\left(1-\beta^m\right)}{\tan^2\varphi + \left(\eta_{rev}^2 - 2\eta_{rev}\eta\right)\left(1-\beta^m\right)} \right]^B \tag{4.9.b}$$

The stress strain relationship for states inside the plastic surface where continuous plastic deformation occurs is expressed by Eq. (4.5). In the cyclic response, the plastic component can be changed to Eq. (4.10).

-Isotropic condition

$$\left(\frac{\partial\eta}{\partial\gamma}\right)^p = \lambda\left\{1-\left[sign(\eta,\Delta\gamma)\eta^3C^2\Delta\gamma\right]\left[1-DC\right]\right\}\left[\frac{1}{C} - sign(\eta_{rev},\Delta\gamma)D\eta_{rev}\Delta\gamma\right]\left\|\frac{1}{\eta-\eta_{rev}}\right\| \tag{4.10.a}$$

-Anisotropic condition

$$\left(\frac{\partial \eta}{\partial \gamma}\right)^{p} = \lambda\left\{1-\left[sign(\eta,\Delta\gamma)\eta^{2}C^{2}\right]\left[1-DC\right]\right\}\left[\frac{1}{C}-sign(\eta_{rev},\Delta\gamma)D\right]\left\|\frac{1}{\eta-\eta_{rev}}\right\| \qquad (4.10.b)$$

Where, $C=\dfrac{\sqrt{\left(1-\beta^{m}\right)}}{\tan\varphi}$, $D=\max\left(\eta,\eta_{rev}\right)$

λ = a material parameter controlling the accumulation of plastic strain as a function of the number of cycles.

Fig. 4.5 and 4.6 shows the flow chart for cyclic test modeling with stress or strain control response, respectively. The procedures of the coding for cyclic response model use the same concept as the monotonic model.

4.4 CONCLUSIONS

The original SIMPLE DSS model described in chapter II was presented in detail in this chapter. The results of direct simple shear tests on Young Bay Mud (YBM) also reviewed and discussed about the strain rate for both monotonic and cyclic test in chapter III. In spite of the importance of strain rate effects on soil response, the SIMPLE DSS model did not treat this issue. The relationships between undrained shear strength and log scale of strain rate are already defined. The proposed model in this chapter attempts to investigate the response of cohesive soil using modified SIMPLE DSS model which includes the strain rate effects in simple shear.

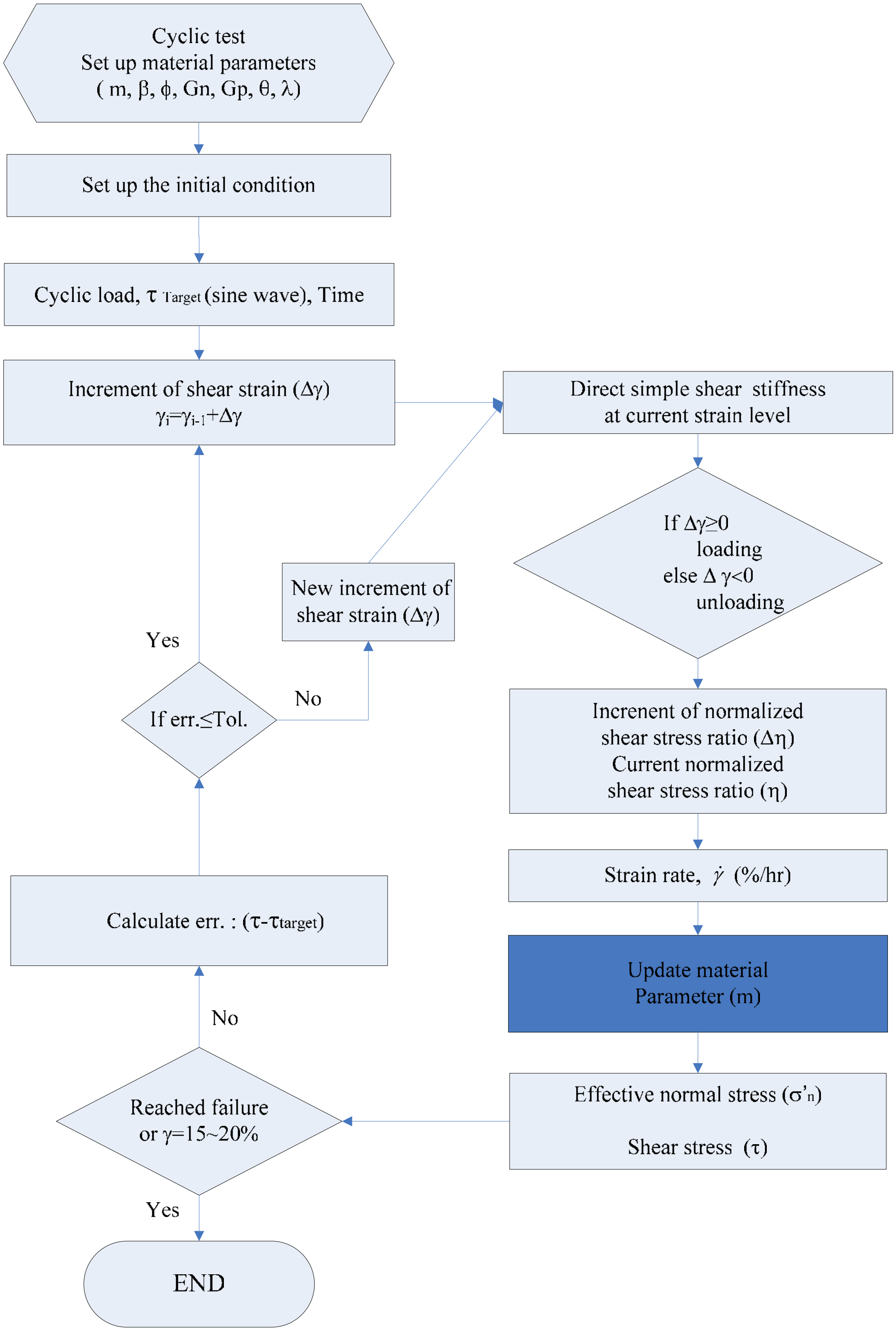

Fig. 4.5. Flow Chart of Modeling of Cyclic Response (Stress-Controlled Test)

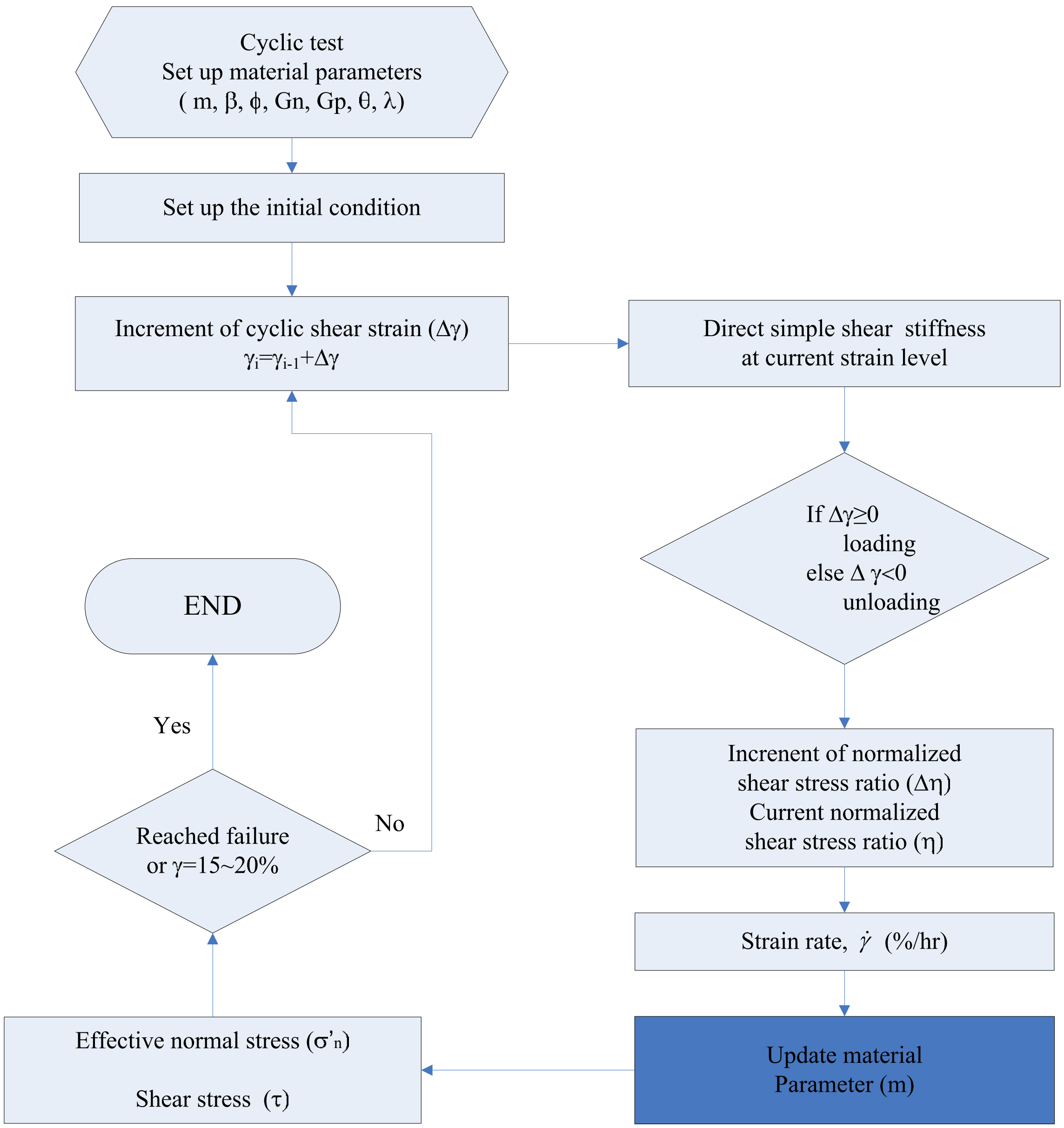

Fig. 4.6. Flow Chart of Modeling of Cyclic Response (Strain-Controlled Test)

CHAPTER V

MODEL VERIFICATIONS

5.1 GENERAL

The modified SIMPLE DSS model was introduced and discussed in the previous chapter. The model takes into account the effect of strain rate both in monotonic and cyclic tests in direct simple shear. This chapter evaluates the predicted response for the undrained simple shear behavior of cohesive soils with modified SIMPLE DSS model. The calibration of material parameters is discussed and predictions are compared with data for two different types of clay: Boston Blue Clay (BBC) from Malek (1987) and Young Bay Mud (YBM) from Biscontin (2001). Both experimental programs were based on direct simple shear tests.

5.2 MONOTONIC RESPONSE

5.2.1 Boston Blue Clay (BBC)

Boston Blue Clay (BBC) long been investigated by many researchers has the largest amount of data in monotonic and cyclic tests. In spite of the large amount of data, there are just few data on monotonic tests with varying strain rates. The relationship of peak shear strength and normalized strain rate was proposed by many researchers. Sheahan et al. (1996) performed series of triaxial test on Boston Blue Clay with several strain rates. Table 5.1 shows the results of consolidated undraied compression tests on normally consolidated Boston Blue clay. They introduce a strain-rate parameter ($\rho_{\dot{\gamma}}$) in strength with change in strain rate.

Table 5.1. Results of Tests on BBC (Sheahan et al., 1996)

Test no. (1)	σ'_{vci} kPa $(K_o)^a$ (2)	OCR (3)	$\dot{\varepsilon}_a{}^b$ (%/h) (4)	At Peak Shear Stress ε_a (%) (5)	q/σ'_{vc} (6)	p'/σ'_{vc} (7)	$\Delta u_s/\sigma'_{vc}{}^c$ (8)	ϕ' (9)	At Maximum Obliquity ε_a (%) (10)	q/σ'_{vc} (11)	p'/σ'_{vc} (12)	ϕ' (13)
CTX-21	284 (0.478)	1.00	0.051	0.22	0.298	0.734	0.018	23.9°	8.70	0.274	0.514	32.1°
CTX-23	291 (0.490)	1.00	0.051	0.37	0.300	0.716	0.045	24.8°	9.87	0.277	0.503	33.4°
CTX-11	281 (0.472)	1.00	0.50	0.13	0.325	0.757	0.023	25.4°	10.97	0.252	0.450	34.0°
CTX-13	276 (0.489)	1.00	0.50	0.18	0.319	0.765	0.003	24.6°	12.18	0.247	0.455	32.9°
CTX-33	293 (0.518)	1.00	5.0	0.21	0.342	0.806	−0.012	25.1°	12.76	0.240	0.457	31.6°
CTX-17	276 (0.491)	1.05	50	0.39	0.379	0.816	−0.049	27.7°	7.84	0.315	0.564	34.0°
CTX-18	280 (0.487)	1.05	49	0.41	0.374	0.774	−0.015	28.9°	8.17	0.298	0.547	33.1°
CTX-52	292 (0.476)	1.00	49	0.33	0.373	0.806	−0.015	27.5°	7.71	0.295	0.559	31.8°

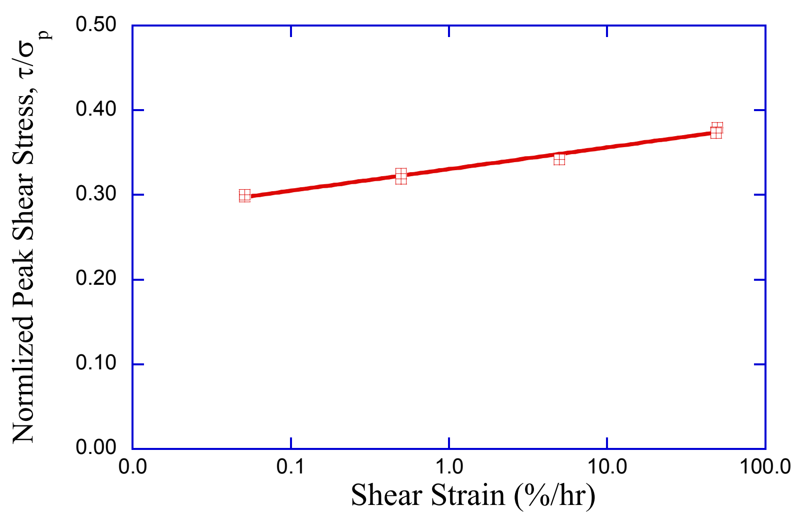

Fig. 5.1. Normalized Shear Strength versus Strain Rate (BBC)

In chapter IV, the literature review showed that the strength increase with strain can be described by a log-linear law. The parameter defining the rate of increase in

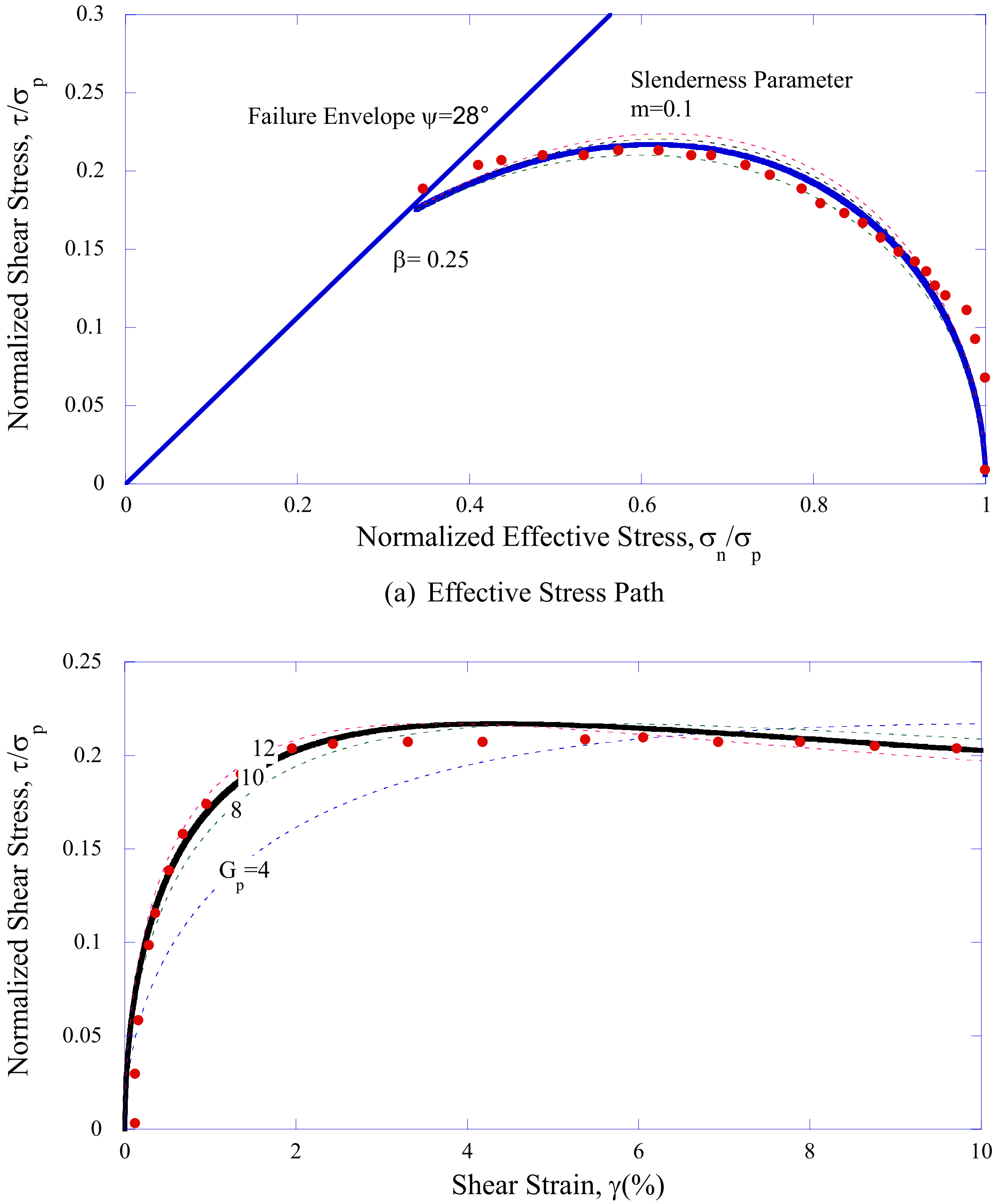

(a) Effective Stress Path

(b) Stress-Strain Curve

Fig. 5.2. Selection of Input Parameters for Monotonic Response of BBC

strength is estimated from experimental results of BBC (see Fig. 4.1.). As shown in Fig. 5.1, the average value of the gradient $\rho_{\dot{\gamma}}$ is 8%. The peak shear stress is obtained from the actual experimental data for a known strain rate. In Malek's monotonic tests, the peak normalized shear stress was about 0.21 corresponding to m=0.1 at standard strain rate (5%/hr). The input material parameters obtained from a short parametric study for monotonic test are summarized in Fig 5.2 and table 4.2.

Table 5.2. Input Parameters for Monotonic Response on Boston Blue Clay (BBC)

Parameter	SIMPLE DSS Biscontin (2001)	Modified SIMPLE DSS
β	0.32	0.32
m	-0.25	0.1
ψ	28	28
G_n	450	450
G_p	8.5	10
$\rho_{\dot{\gamma}}$(%)	-	8

The predicted model performance of the modified SIMPLE DSS was evaluated by comparing with the measured response of Boston Blue Clay. Fig.5.3 shows the result of comparison between estimated result and measured data of a monotonic test on Boston Blue Clay used to define the basic input material parameters, including effective stress path and stress-strain curve. The selection of material parameters in effective stress path is very good, but in stress-strain curve is not good especially at the large strain condition (γ=15~20%). Fig. 5.4 shows the predictions for several strain rates based on the selected material parameters. The normalized shear stress versus strain curves at several high and slow rates of strain show higher shear strength at high strain rate.

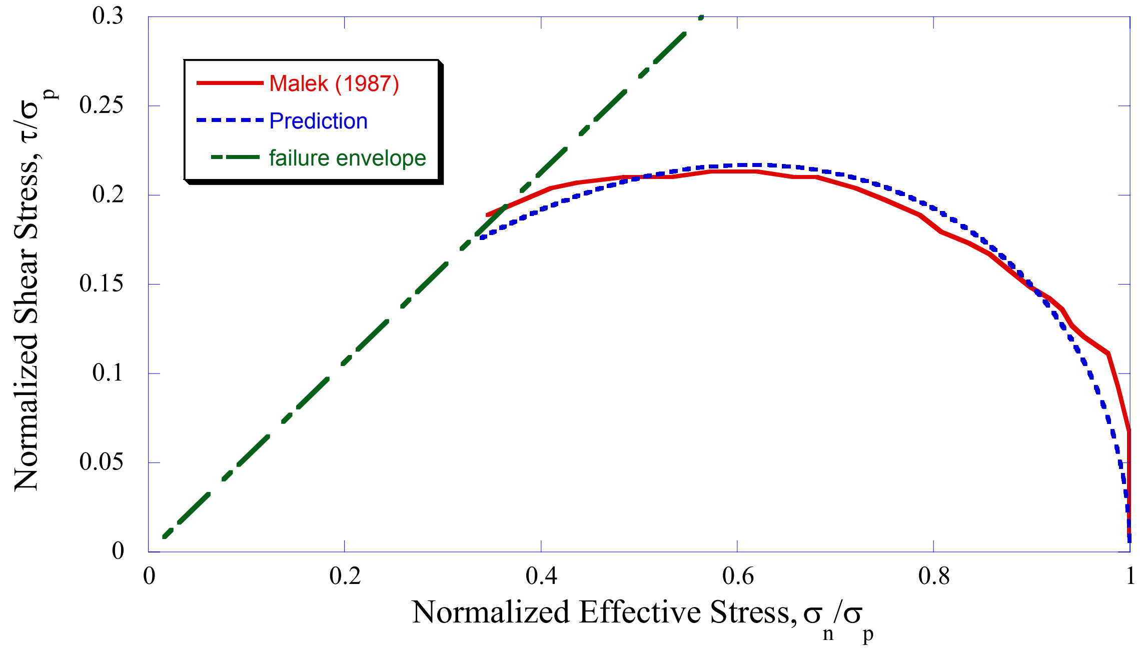

(a) Effective Stress Path

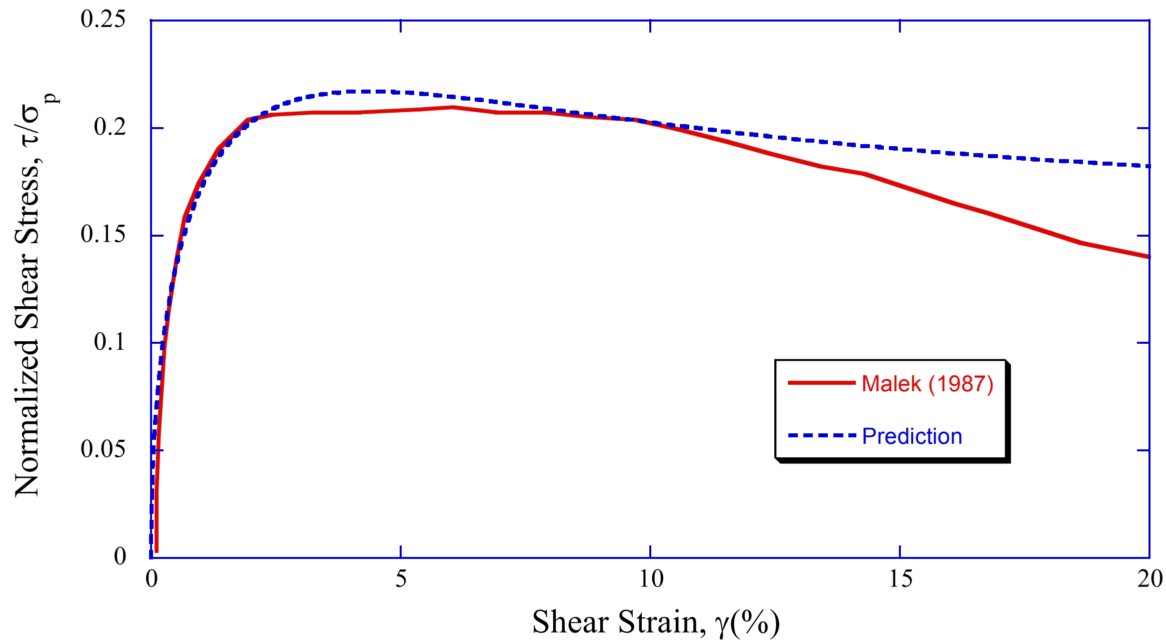

(b) Stress-Strain Curve

Fig. 5.3. Evaluation of Material Parameters for Monotonic Test
(data from Malek,1987)

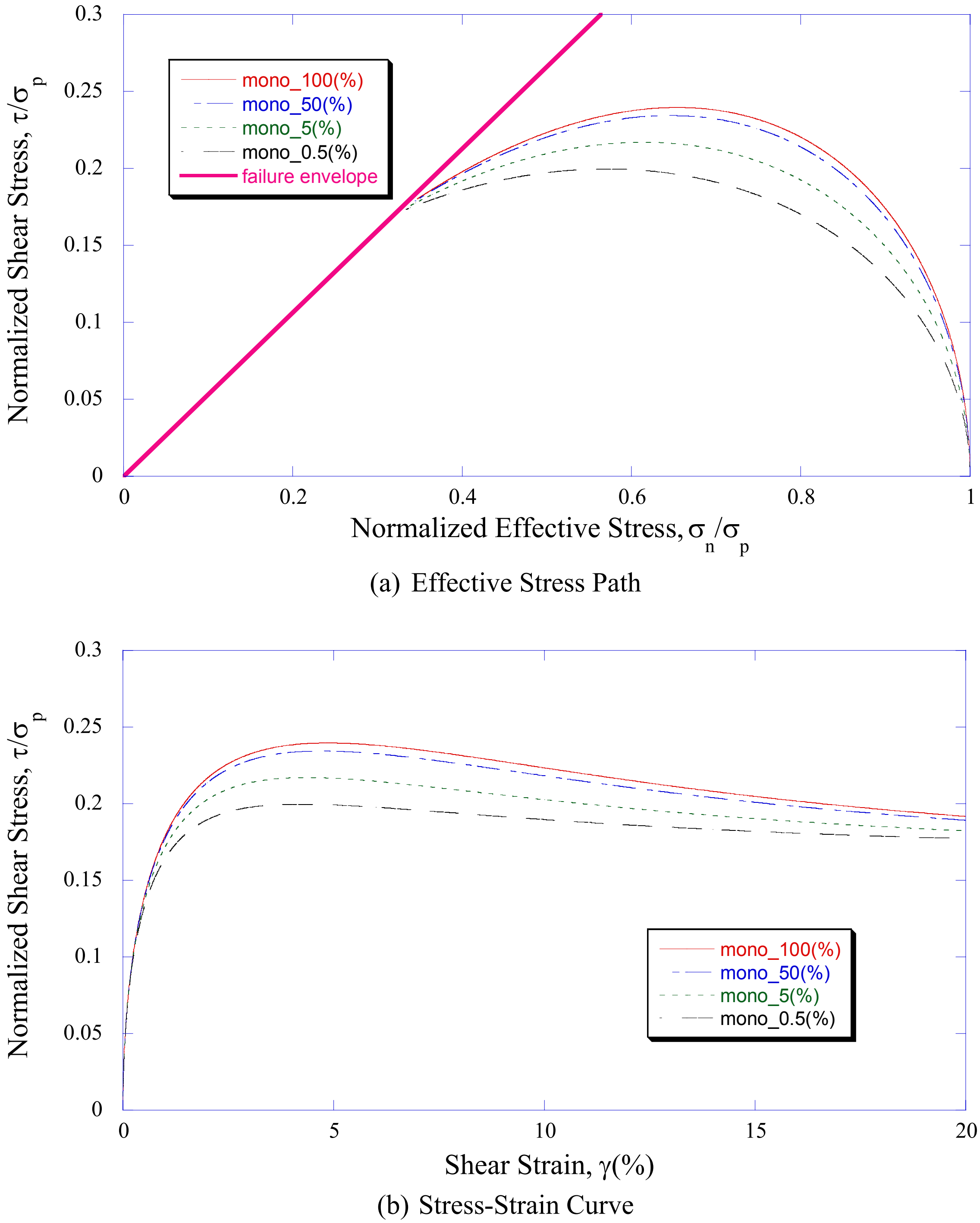

Fig. 5.4. Estimation of Results on Several Strain Rates with Modified SIMPLE DSS (Boston Blue Clay)

5.2.2 Young Bay Mud (YBM)

The behavior of Young Bay Mud has long been investigated. However, the size of the experimental database is much smaller and than that of Boston Blue Clay. The testing program was reviewed in chapter III. The parameters for monotonic response were used to predict the behavior of Young Bay Mud.

Table 5.3. Input Parameters for Monotonic Response on Young Bay Mud (YBM)

Parameter	SIMPLE DSS Biscontin (2001)	Modified SIMPLE DSS
β	0.59	0.59
m	0.75	0.75
ψ	25	25
G_n	350	350
G_p	11	11
$\rho_{\dot{\gamma}}(\%)$	-	11.1

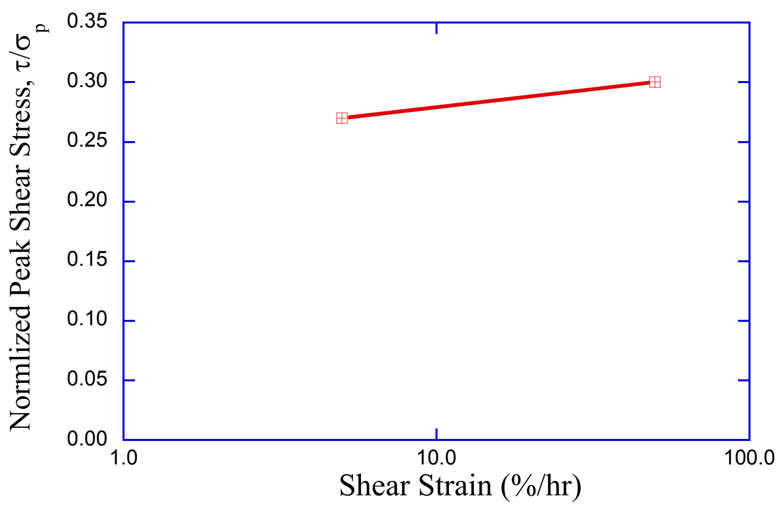

Fig. 5.5. Normalized Shear Strength versus Strain Rate (YBM)

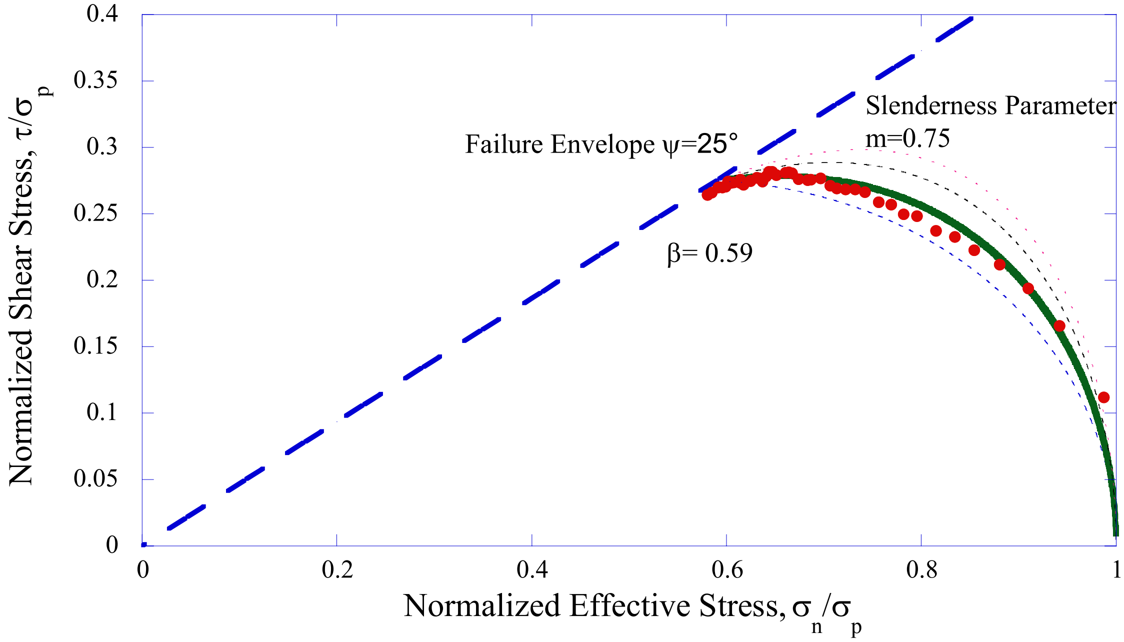

(a) Effective Stress Path

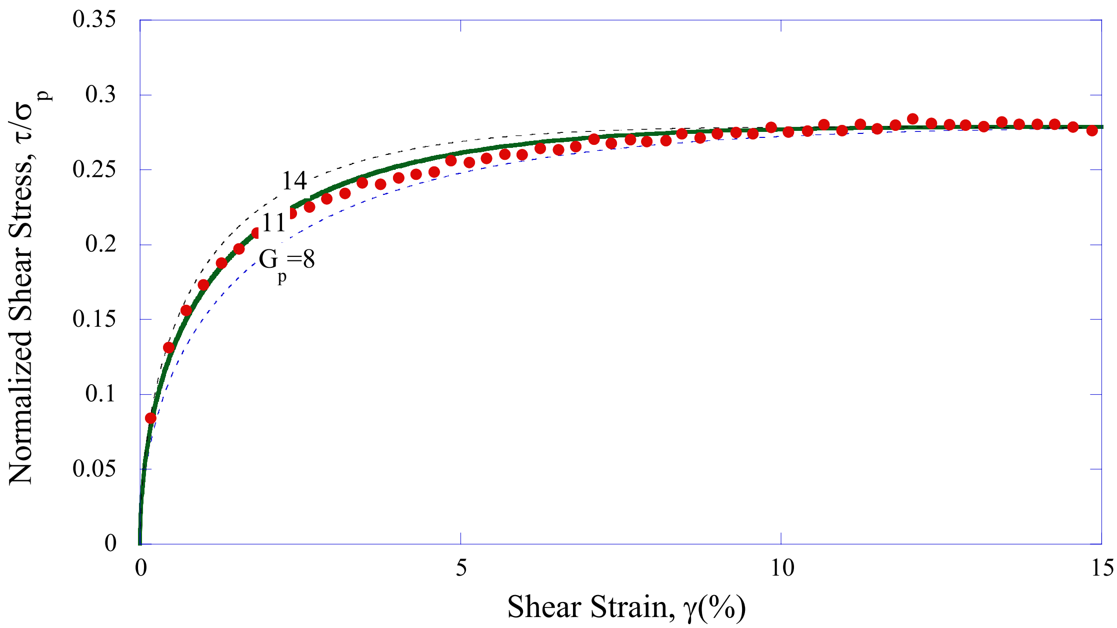

(b) Stress-Strain Curve

Fig. 5.6. Selection of Input Parameters for Monotonic Response of YBM

Table 5.3 and Fig. 5.6 show the selected material parameters based on the work of Biscontin (2001). Additionally, Fig 5.5 shows the selection of strain-rate parameter using the results of the two tests available with strain rate 5% and 50%/hr.

Figs 5.7-5.9 present the response of the Young Bay Mud under different loading conditions. Fig 5.7 shows comparison of the effective stress path and stress strain curve for two tests with rate of strain 5% and 50%/hr between predicted and measured responses. The prediction of the effective stress and stress-strain curves for the 50%/hr strain rate shows reasonable agreement with tested results. Fig 5.8 describes the predicted response with strain rate based on specific material parameter, m, defined by test of standard strain rate. In anisotropic condition, this model also can capture the soil behavior without changing material parameter, m (see Fig. 5.9). The model is able to capture the increase in shear strength with increasing strain rate without changing m.

If soil were subjected to irregular loading such as seismic, wind, or vibration loading, the behavior of soil would still depend on rate of strain. Fig 5.10 shows the response of the soil element subjected irregular loading. In a monotonic test, the initial shear modulus is defined by the gradient of straight line of the shear stress versus shear strain relationship. At the first small strain, the shear modulus is too large because there is only elastic component. Richardson and Whitman (1963) introduced a novel testing known as step-changed method to study the effect of strain rate on the undrained shear strength (see Fig. 2.3). Fig 5.11 shows the response of the soil element subjected step-changed loading. The responses for irregular and step-changed loading are also affected by the strain rate.

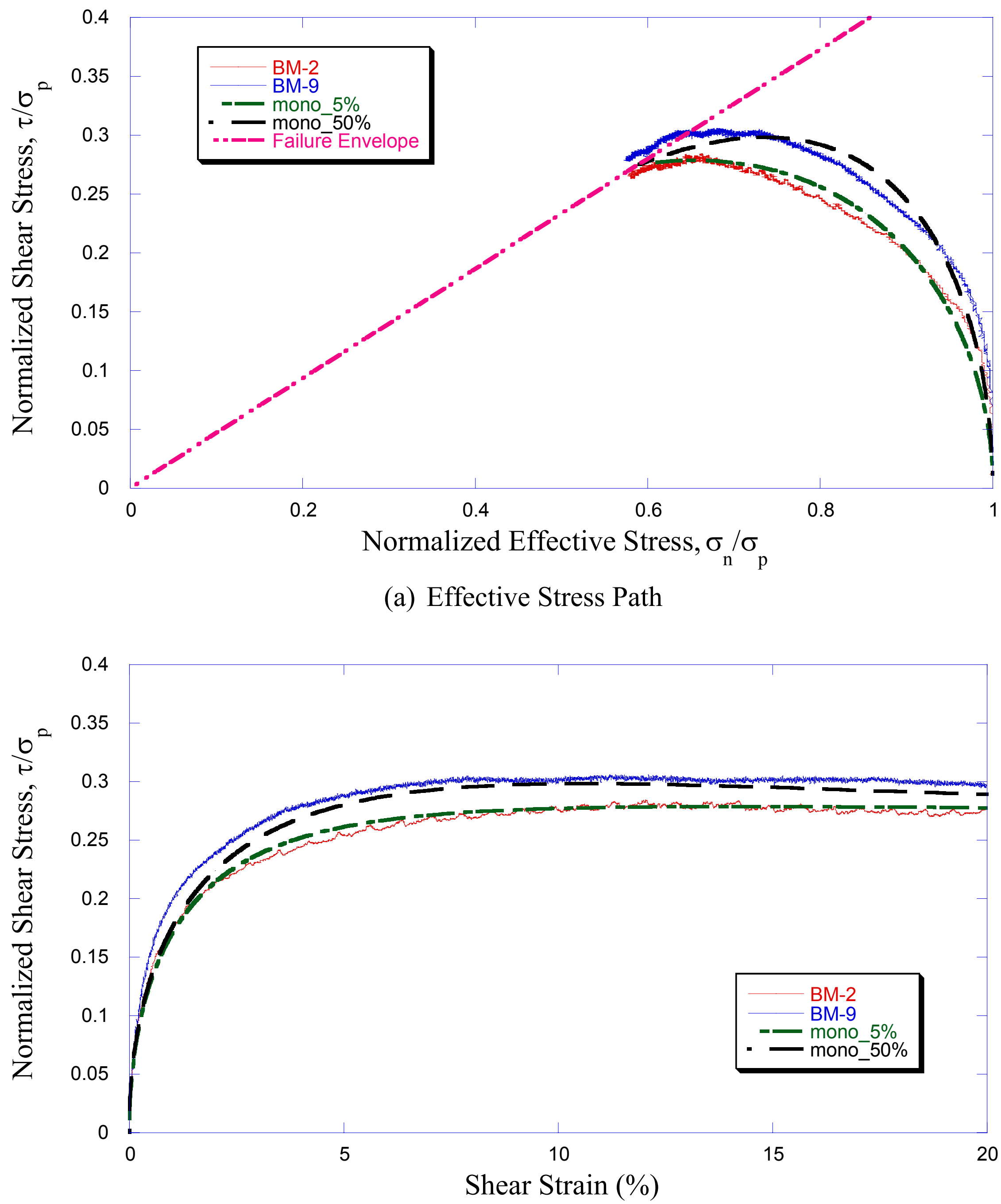

(a) Effective Stress Path

(b) Stress-Strain Curve

Fig. 5.7. Comparison of the Results with Measured Data
(data from Biscontin, 2001)

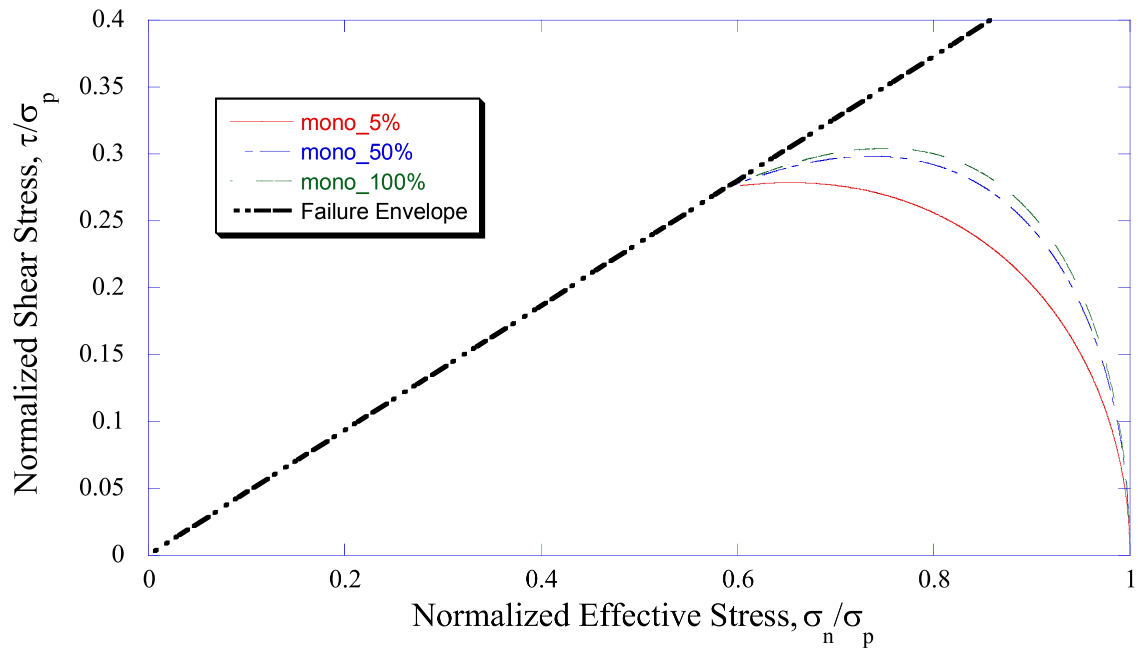

(a) Effective Stress Path

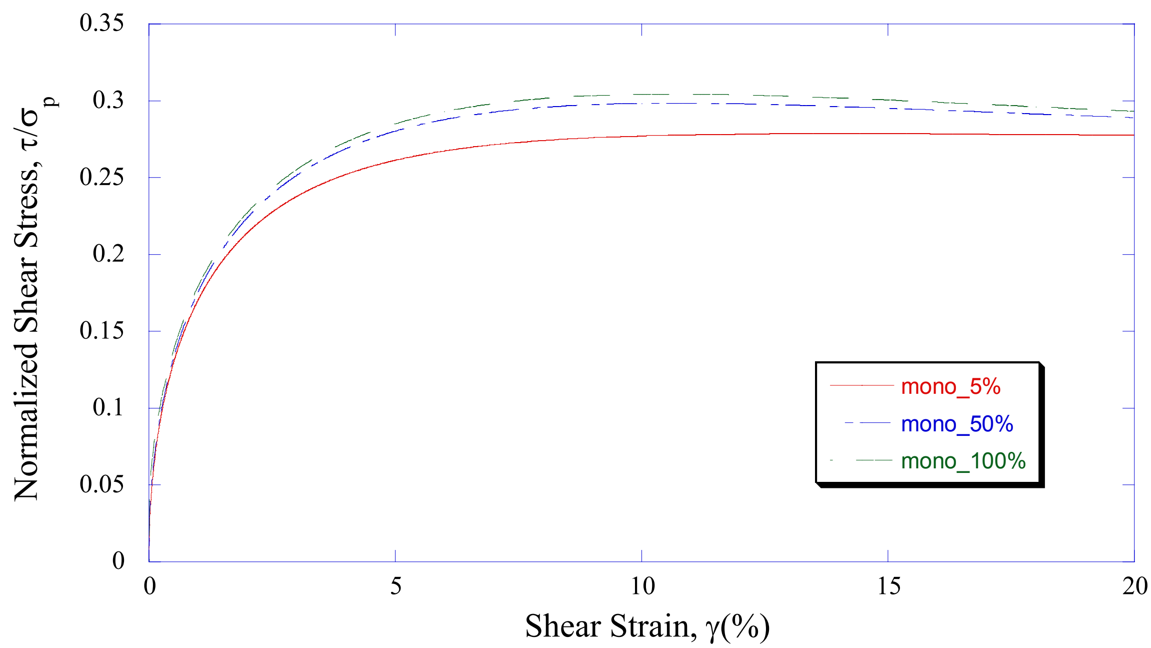

(b)Stress-Strain Curve

Fig. 5.8. Estimation of Results on Several Strain Rates with modified SIMPLE DSS (Young Bay Mud)

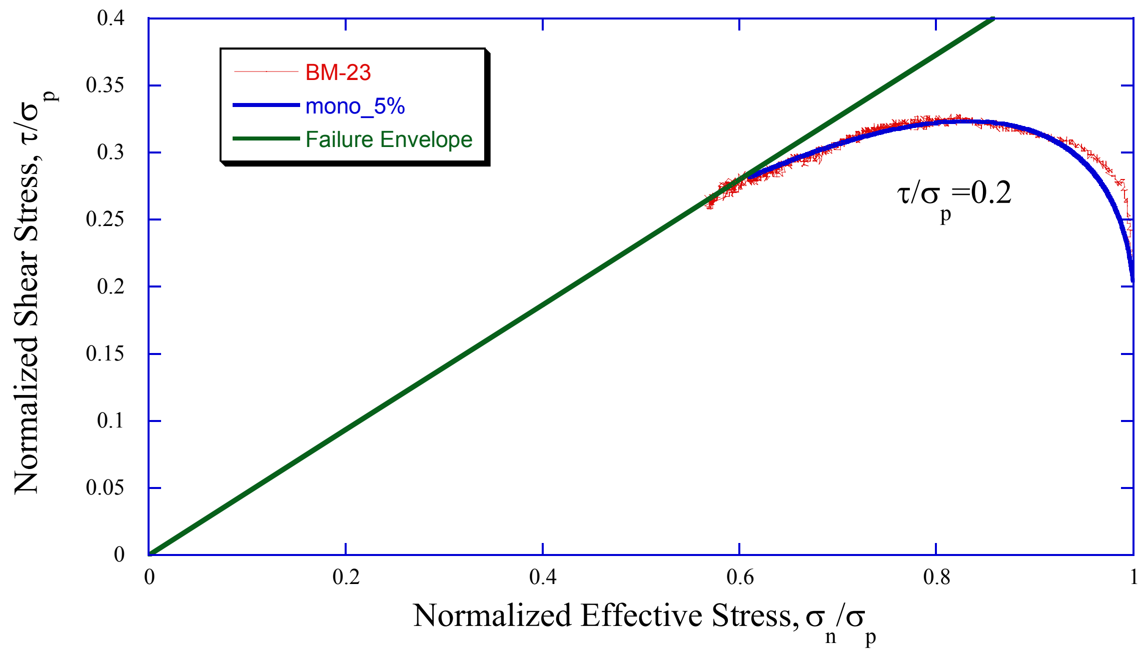

(a) Effective Stress Path

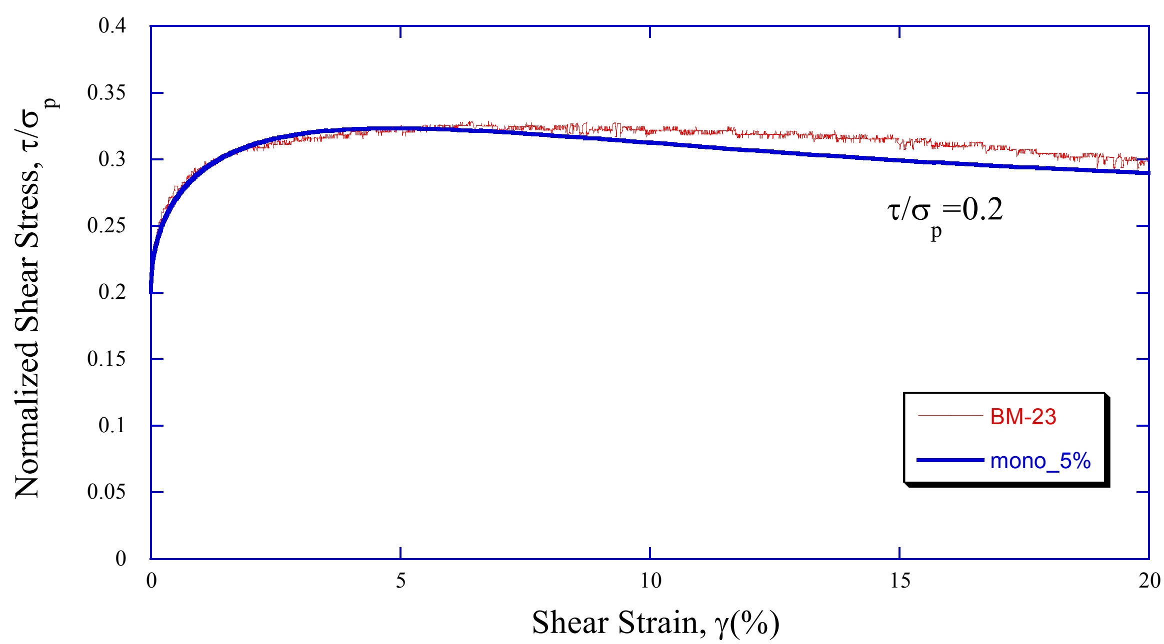

(b) Stress-Strain Curve

Fig. 5.9. Estimation of Results with Modified SIMPLE DSS on Anisotropic Consolidation (Young Bay Mud)

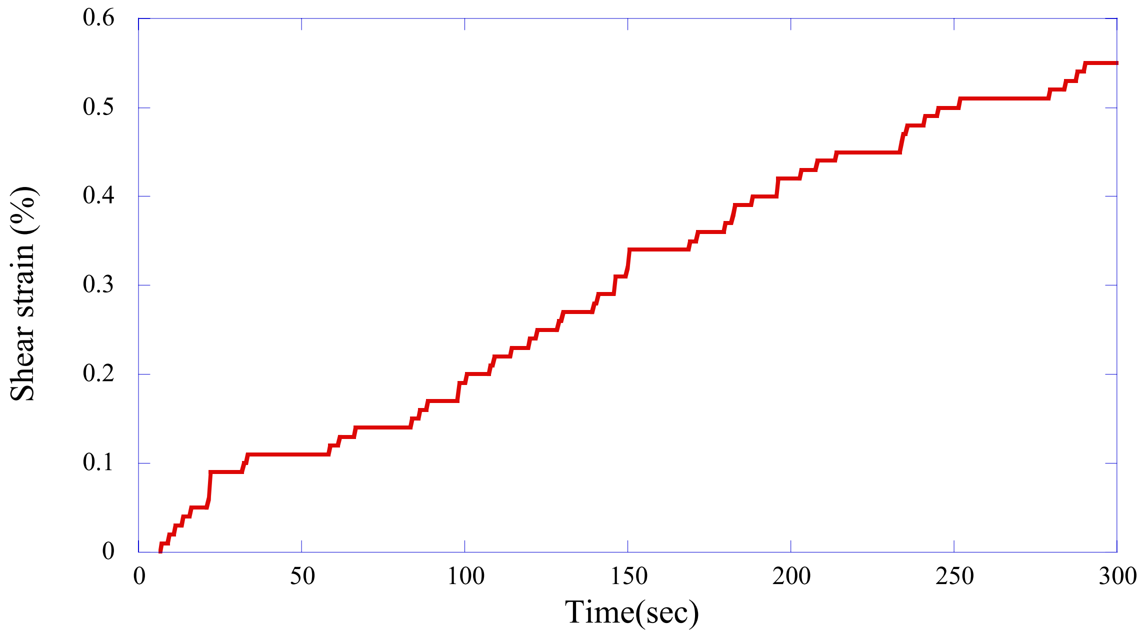

(a) Time-Shear Strain

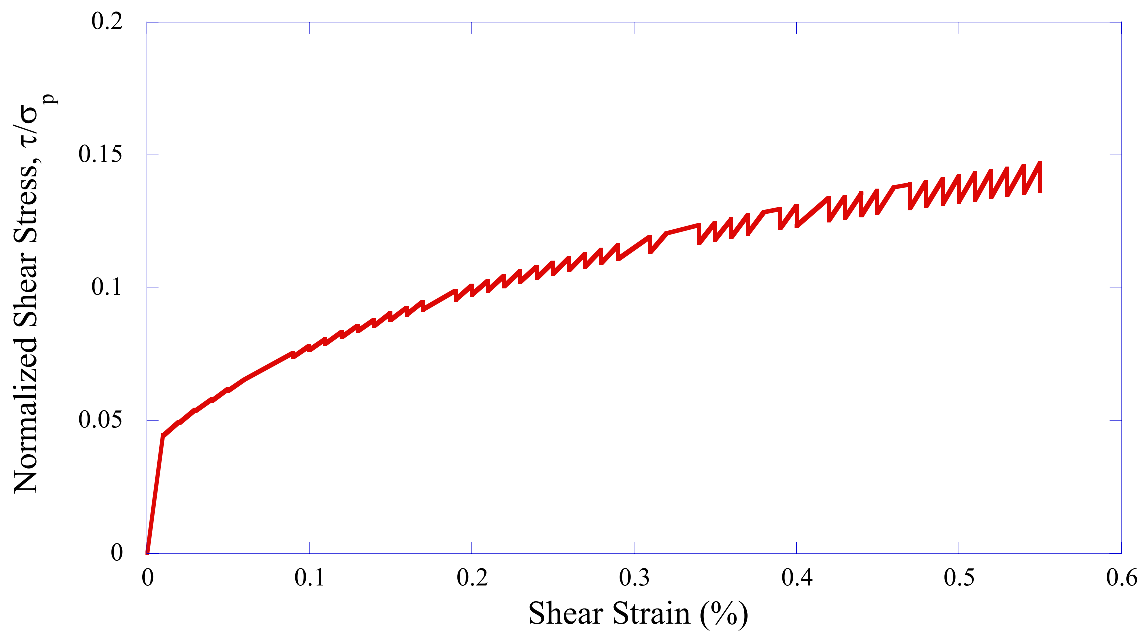

(b) Stress-Strain Curve

Fig. 5.10. Estimation Response to Irregular Loading Condition

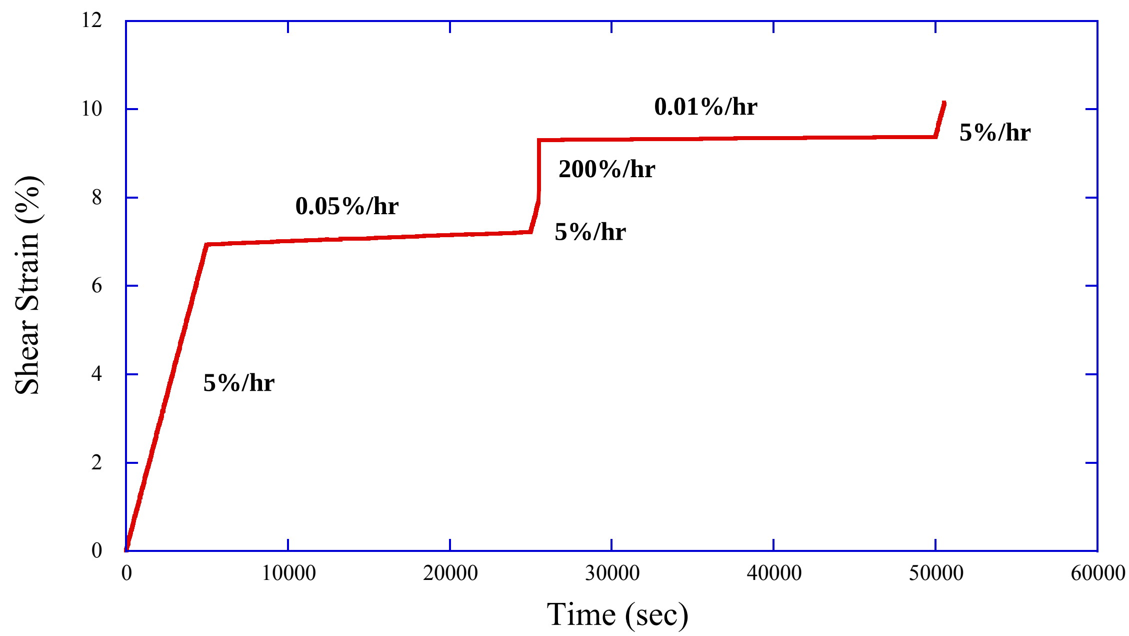

(a) Time-Shear Strain

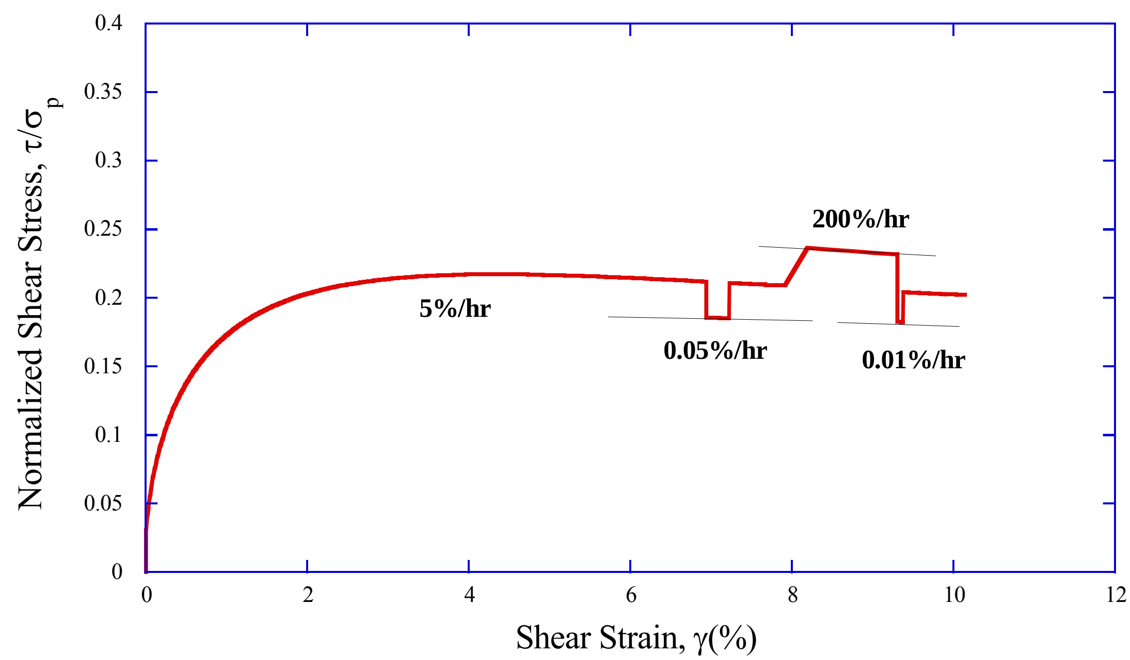

(b) Stress-Strain Curve

Fig. 5.11. Estimation Response of Step-Changing Test

5.3 FIRST LOADING IN CYCLIC RESPONSE

This section present the results of predicted responses aimed at developing a better understanding of strain rate effects on clay behavior under cyclic loading. In chapter III, the results for both cyclic and monotonic tests were presented to define the rate of effects in cyclic simple shear tests (see Fig. 3.7 and 3.8). The cyclic behavior is a highly affected with strain rate effects.

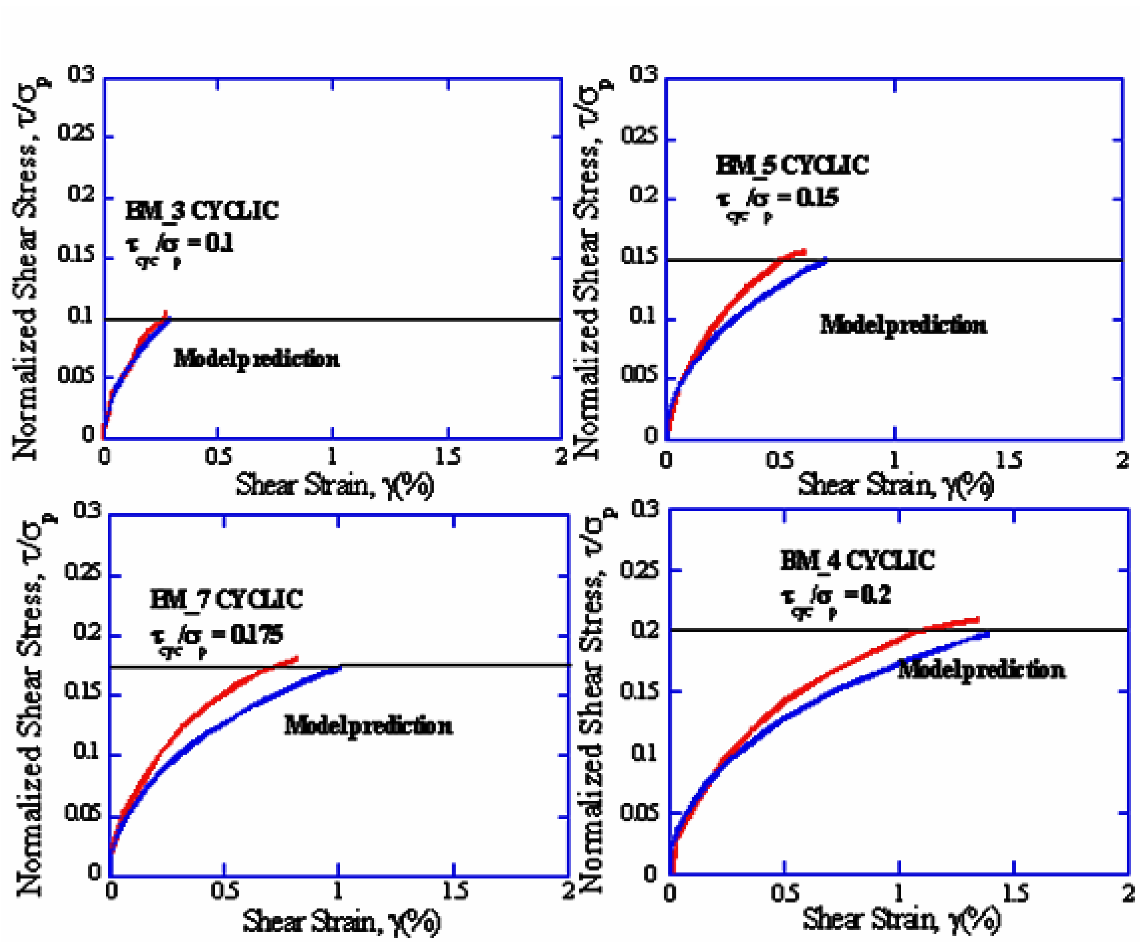

Fig. 5.12. Evaluation of Cyclic Responses with Predicted and Measured Data

Fig. 5.12 and table 5.4 show the results of model prediction with measures response of shear stress versus shear strain under cyclic loading just considering the first cycle. The development of shear stain during the test is in good agreement at lower cyclic shear stress ratio (CSR). In the contrast, differences with measured and predicted increase with increasing the cyclic shear stress ratio (CSR).

Table 5.4. Results of Model Prediction

Test	Consolidation Shear Stress (τ_c/σ_p)	Cyclic Shear Stress Ratio (τ_{cyc}/σ_p)	Measured Strain Rate (%/hour)	Predicted Strain Rate (%/hour)
BM-3	0.00	0.100	389	412
BM-4	0.00	0.200	1930	1993
BM-5	0.00	0.150	864	1005
BM-7	0.00	0.175	1166	1440

CHAPER VI

SUMMARY, CONCLUSIONS AND RECOMMENDATION

6.1 SUMMARY

This thesis presents work on modeling of the effect of strain rate on direct simple shear test results, comparing experimented results and computational response of monotonic and cyclic tests. The modeling program was implemented in Matlab in order to illustrate the general behavior of cohesive soils and to provide the modeling of the soil behavior based on the calibration of a SIMPLE DSS model.

6.2 CONCLUSIONS

The objective of this research is the development of new model to describe the behavior of cohesive soils under time dependent loading. The modified SIMPLE DSS model includes the effects of strain rate on clays in simple shear. The first step of the work was to define the unique relationship that would provide a general relationship between shear strength and strain rate. The section on literature review describes a number of approaches that define the relationship in terms of shear strength and log scale of strain rate so that model included this conventional concept.

The development of the model requires implementation and computer coding. The original SIMPLE DSS model was an effective stress and rate independent model for the prediction of the response of cohesive soils in simple shear. The model required seven input material parameters, five for the monotonic and two for cyclic behavior. All these parameters have specific function in the model response. The proposed model, a modified SIMPLE DSS, focuses on one material parameter, referred as slenderness parameter (m), because it mostly controls the undrained shear strength. Since the undrained shear strength depends on the strain rate, controlling the slenderness material parameter provides a convenient way to link strain rate and strength.

Finally, the proposed model evaluation was carried out comparing the model responses and results of simple shear tests on Boston Blue Clay (Malek, 1987) and Young Bay Mud (Biscontin, 2001). The model capability is evidenced in the comparing by strain rate dependent responses for both monotonic and cyclic behavior. For the monotonic tests, the model predictions show general agreement with the data, for both Boston Blue Clay and Young Bay Mud. The proposed model is able to predict the increase in undrained shear strength for higher strain rates.

Base on the theoretical and modeling investigation of strain rate effects on undrained shear strength of clay in simple shear, the following can be concluded.

1. Undrained shear strength in simple shear is directly related to strain rate effects. A higher strain rate results in higher undrained shear strength.
2. The responses in cyclic test show the more dependent behavior than those in monotonic test.
3. Undrained shear strength increase as about 11% for tenfold change in log scale of strain rate for Young Bay Mud (YBM).
4. The proposed model can capture the response of irregular loading and step-changed conditions.

6.3 RECOMMENDATION FOR FUTURE WORK

A typical lack of information prevents an extensive comparison of predictions with actual measured soil response. For this reason, additional laboratory tests are needed to characterize the general relationship between shear strength and strain rate, similar to earthquake rates, for example especially in the higher range of strain rate. Yong and Japp (1967) concluded that the relationship between shear strength and log scale of strain rate is bilinear at extremely high strain rate. For cyclic tests, the strain rate effects are more pronounced than for monotonic tests. This will help in understanding the shear strength of cohesive soils for new modeling.

REFERENCES

Andersen, K. (1991) “Foundation Design of Offshore Gravity Structures.” *Cyclic Loading of Soils*, M. P. O. Reilly and S. F. Brown eds., Blackie, New York, 122-171.

Awoleye, O.A., Bouazza,A., and Rama-Rao,R. (1991). “Time Effects on the Unconfined Compressive Strength and Sensitivity of Clay.” *Eng. Geology,* 31(3-4), 345-351.

Biscontin, G. (2001). “Modeling the Dynamic Behavior of Lightly Overconsolidated Soil Deposits on Submarine Slope.” *PhD dissertation*, University of California, Berkeley.

Biscontin, G. and J.M. Pestana (1999). “Influence of Peripheral Velocity on Undrained Shear Strength and Deformability Characteristic of a Bentonite-Kaolinite Mixture.” *Technical Report* UCB/GT/99-19, University of California, Berkeley.

Casagrande, A. and Carrillo, N. (1994). “ Shear Failure of Anisotropic Materials.” *Proc., Boston Soc. Civ. Eng.,* 31. 74-87.

DeGroot, D. (1989). “The Multidirectional Direct Simple Shear Apparatus with Application to Design of Offshore Arctic Structures. *Sc.D. Thesis*, Massachusetts Institute of Technology, Cambridge.

Denby, G. (1978). “Self Boring Pressuremeters Study of San Francisco Bay Mud.” *Technical Report* CE-232, Dept. of Civ. Eng. Stanford University, Palo Alto, CA.

Duncan, J (1965). “The Effects of Anisotropy and Reorientation of Principal Stresses on the Shear Strength of Saturated Clays.” Ph.D. University of California, Berkeley.

Graham, J., Crooks, J.H. A., and Bell, A.L. (1983). “Time Effects on the Stress-Strain Behavior of Soft Natural Clays.” *Géotechnique*, 33(3), 327–340.

Housel, W. S. (1960). “Dynamic and Static Resistance of Cohesive Soils 1846-1958.” *Papers on soils-1959 Meetings, Symposium on Time Rates of Loading in Soil Testing ASTM Special Technical Publication No.254*, Philadelphia, 4-35.

Idriss, I.,R. Dorby, and R. Singh (1978). “Nonlinear Behavior of Soft Clay during Cyclic Loading.” *J. Geotec. Eng.,* 104(12), 1427-1447.

Katti, D.R., Tang, J.P., and Yazdani, S. (2003). “Undrained Response of Clays to Varying Strain Rate.” *J. Geotec. Geoenviron. Eng.,* 129(3), 278-282.

Konard, J. M., and Wagg, B. T. (1993). “Undrained Cyclic Loading of Anisotropically Consolidated Clayey Silts.” *J. Geotech. Eng. Div., Am. Soc. Civ. Eng.,* 119(5), 929– 947.

Ladd, C. (1991). “Stability Evaluation during Staged Construction.” *J. Geotec. Eng.,* 117(4), 540-615.

Lefebvre, G., and LeBoeuf, D., (1987). “Rate Effects and Cyclic Loading of Sensitive Clays.” *J. Geotec. Geoenviron. Eng.,* 113(5), 476-489.

Luccioni, L. (1999). “Numerical Development and Implementation of a Constitutive Model for Clays with Application to Deformation around a Deep Excavation.” *PhD dissertation*, University of California, Berkeley.

Malek, A. (1987). “Cyclic Behavior of Clay in Undrained Simple Shearing and Application to Offshore Tension Piles.” *Sc.D. Thesis*, Massachusetts Institute of Technology, Cambridge.

Matesic, L. and Vucetic, M. (2003). “Strain-Rate Effect on Soil Secant Shear Modulus at Small Cyclic Strains.” *J. Geotec. Geoenviron. Eng.,* 129(6), 536-549.

Mayne, P. W. (1985). “A Review of Undrained Strength in Direct Simple Shear.” *Soils Found.,* 25(3), 64-72.

Murakami, S., Yasuhara, K., andBessho, K. (1996). “Predition of Time-dependent Behavior of Remolded Soft Marine Clay in Axi-Symmetric Undrained Conditions.” *Geotechnical Special Publication*, n 61, *Measuring and Modeling Time Dependent Soil Behavior*, T. C. Sheahan and V. N. Kaliakin eds., ASCE, 181-194.

Perloff, W. H (1962). “The Effect of Stress History and Strain Rate on the Undrained Shear Strength of Cohesive Soils.” *PhD dissertation*, Northwestern University, Evanston.

Pestana, J.M., G. Biscontin, F. Nadim, and K. Andersen (2000). “Modeling Cyclic Behavior of Lightly Overconsolidated Clays in Simple Shear.” *Soil Dynamics and Earthquake. Eng.,* 19, 501-519.

Prevost, J. H. (1979). “Undrained Shear Tests on Clays.” *J. Geotech. Eng. Div., Am. Soc. Civ. Eng.,* 105(1), 49-64.

Rau, G. (1999). “Evaluation of Strength Degradation in Seismic Loading of Holocene Bay Mud from Marine County, California.” *PhD dissertation*, University of California, Berkeley.

Richardson, A. M., and Whitman, R. V. (1963). “Effect of Strain Rate upon Undrained Shear Resistance of a Saturated Remolded Fat Clay.” *Géotechnique*, 13, 310–324.

Sheahan, T. C., Ladd, C. C., and Germaine, J. T. (1996). “Rate-Dependent Undrained Shear Behavior of Saturated Clay.” *J. Geotech. Eng.*, 122(2), 99-108.

Yong, R. N., and Japp, R. D. (1967) “A Flow Law for Clays in Dynamic Compression.” *Proc., Int. Symposium on Wave Propagation and Dynamic Properties of Earth Materials*, University of New Mexico Press, Albuquerque, 183-188.

Yue, Dongyi (2001). “An Anisotropic and Time-Dependent Bounding Surface Model for Clays and its Application to a Containment System Constructed over a Soft Foundation.” *PhD dissertation*, Columbia University, New York.

Zhu, J.-G., and Yin, J,-H. (2000). “Strain-Rate-Dependent Stress-Strain Behavior of Overconsolidated Hong Kong Marine Clay.” *Canadian Geotech. J.,* 37(6), 1272-1282.

APPENDIX A

CODING OF MODIFIED SIMPLE DSS MODEL

MONOTONIC RESPONSE

```
clear all
clf

%%% beta: Failure Ratio Parameter %%%
%%% m: Slenderness Parameter      %%%
%%% psi: Maximum Obliquity         %%%
%%% Gn: Describe(Gmax/sigma)      %%%
%%% Gp: Describe the first loading%%%

beta=0.32;
m=0.1;
psi=28;
Gn=450;
Gp=10;

tanpsi=tan(psi*pi/180);
one_b=1-beta^m;
bm=beta^m;

%%% Define the reference strength %%%
A= sqrt(1/((1-beta^m)*(1+2/m)));
Suref= A*(2/(2+m))^(1/m)*tanpsi;
%%%%%%%%%%%%%%%%%%%%%%%%%%%%%%%%%%%%%

rho=0.08;    %%% Strain Rate Parameter %%%%
gref=5;      %%% Reference Strain rate %%%%
g1=0.5;      %%% Specific strain rate  %%%%

%%% set up the IC %%%%
sn0=1.0;
tau0= 0;
g0=0.0;
n0=tau0/sn0;
na=[n0];
ga=[g0];
sna=[sn0];
taua=[tau0];
ta=[0];
n=n0;
g=g0;
sn=sn0;
tau=tau0;
t=0;

%%%%%%%%%%%%%%%%%  set up strains and time
dt=5;                  %%%%%% time increment
dg=g1/3600/100*dt;     %%%% strain increment
gdot=dg/dt*100*3600; %%%%%%%%in percent/hr
%%%%%%%%%%%%%%%%%%%%%%%%%%%%%%%%%%%%%%%%%%
```

```
%%% First step to avoid divide by zero on first load
Ge=Gn*(sn0/sn)^0.5;
dn=Ge*dg;

n=n+dn;
g=g+dg;
t=t+dt;
m = fzero(@(x) Sum(Suref,rho,gref,gdot,beta,tanpsi,x), m);
sn= sn0*(beta^m+((1-beta^m)*(tanpsi^2-n^2)/(tanpsi^2+0.8*n0^2-
1.8*n0*n)))^(1/m);
tau=sn*n;

ga=[ga,g];
na=[na,n];
sna=[sna,sn];
taua=[taua, tau];
ta=[ta, t];

for k=2:10000   %%% Number of Point %%%%
    E=sign(n*dg);
    Ge=Gn*(sn0/sn)^0.5;
    Gplastic=Gp*(tanpsi-sign(n0*dg)*n0)*(tanpsi-E*n)/(n-n0);
    G=max(10^(-30),(Ge/(1+(Ge/Gplastic))));
    dn=G*dg;
    n=n+dn;
    t=t+dt;
    gdot=dg/dt*100*3600;
    m = fzero(@(x) Sum(Suref,rho,gref,gdot,beta,tanpsi,x), m);
    sn= sn0*(beta^m+((1-beta^m)*(tanpsi^2-n^2)/(tanpsi^2+0.8*n0^2-
1.8*n0*n)))^(1/m);
    tau=sn*n;

    g=g+dg;
    ga=[ga,g];
    na=[na,n];
    sna=[sna,sn];
    taua=[taua, tau];
    ta=[ta, t];
end

subplot(2,1,1)
plot(sna,taua,':')%%%% Effective Stress Path %%%
hold on
subplot(2,1,2)
plot(ga,taua)     %%%% Stress-Strain Curve %%%%
hold on
```

Function of Zero

```
function y = Sum(Suref,rho,gref,gdot,beta,tanpsi,x)

if(gdot)<=0.1
     Su = Suref+Suref*rho*log10(0.1/gref);
else
     Su=Suref+Suref*rho*log10((gdot)/gref);
end

A= sqrt(1/((1-beta^x)*(1+2/x)));
y = Su-A*(2/(2+x))^(1/x)*tanpsi;
```

CYCLIC RESPONSE (STRESS-CONTROLLED TEST)

```
clear all
clf

%%% beta: Failure Ratio Parameter %%%
%%% m: Slenderness Parameter      %%%
%%% psi: Maximum Obliquity         %%%
%%% Gn: Describe(Gmax/sigma)      %%%
%%% Gp: Describe the first loading%%%
%%% theta: Accum. of Pore Pressure%%%
%%% lambda: Accum. of Strain      %%%
beta=0.59;
m=0.75;
psi=25;
Gn=350;
Gp=11;

theta=200;
lambda=80;

tanpsi=tan(psi*pi/180);
A= sqrt(1/((1-beta^m)*(1+2/m)));
Suref= A*(2/(2+m))^(1/m)*tanpsi;

rho=0.01;
gref=5;

one_b=1-beta^m;
bm=beta^m;
mparam=[beta,tanpsi,one_b,bm,rho,gref,Suref];

% set up IC
sn0=1.0;
tau0= 0;
g0=0.0;
n0=tau0/sn0;
nrev=n0;
snrev=sn0;
dir=1;

na=[n0];
ga=[g0];
sna=[sn0];
taua=[tau0];
gadot=[];
n=n0;
g=g0;
sn=sn0;
tau=tau0;
```

```
%set up cyclic load, sine wave for shear stress
tcyc=0.1;
T=10; % period of the sine wave in s
N=1;
space=100;
dt=T/space;

t=dt;
dg=0.00003;  % not in percent
err=0.5;
chk=0;
dir=1;
nsurf=1;

% % First step to avoid divide by zero on first load
t=t+dt;
tauT=tcyc*sin(2*pi*t/T);
N=t/10;

Ge=Gn*(sn0/sn)^0.5;

while abs(err)>0.00001
dn=Ge*dg;
n=n0+dn;
gdot=dg/dt*100*3600; %in percent/hr
m = fzero(@(x) Sum(Suref,rho,gref,gdot,beta,tanpsi,x), m);
sn= sn0*(beta^m+((1-beta^m)*(tanpsi^2-n^2)/(tanpsi^2+0.8*n0^2-
1.8*n0*n)))^(1/m);
tau=sn*n;
Ge=Gn*(sn0/sn)^0.5;
err=(tau-tauT);
%recalculate the shear stress due to the error at first step
dg=(dg/abs(tau-tauT0))*abs(tauT-tauT0);
end
g=g+dg;
ga=[ga,g];
na=[na,n];
sna=[sna,sn];
taua=[taua, tau];

for k=2:2000    %number of data points
    t=t+dt;
    tauT=tcyc*sin(2*pi*t/T);
    tauT1=[tauT1, tauT];
    N=t/T;
    err=0.1;
    dg=dg;

   %%%%%% determination of reversal point(nrev and snrev)%%%%%%%%%%
    if abs(tauT)>=tcyc
        nrev=n;
        snrev=sn;
```

```
    end
   %%%%%%%%%%%%%%%%%%%%%%%%%%%%%%%%%%%%%%%%%%%%%%%%%%%%%%%%%%%%%%%%%%

   %%%%%%%%% on plastic bounding surface %%%%%%%%%%%%%%%%%%%%%%%%%%%%
if N<0.25

    E=sign(n*dg);
    Ge=Gn*(sn0/sn)^0.5;
    Gplastic=Gp*(tanpsi-sign(n0*dg)*n0)*(tanpsi-E*n)/(n-n0);
    G=max(10^(-30),(Ge/(1+(Ge/Gplastic))));
    n1=n;

    while abs(err)>0.00001
    dn=G*dg;
    n=n1+dn;
    gdot=dg/dt*100*3600;
    m = fzero(@(x) Sum(Suref,rho,gref,gdot,beta,tanpsi,x), m);
    sn= sn0*(beta^m+(1-beta^m)*(tanpsi^2-n^2)/(tanpsi^2+0.8*nrev^2-
1.8*nrev*n))^(1/m);
    tau=sn*n;
    E=sign(n*dg);
    Ge=Gn*(sn0/sn)^0.5;
    Gplastic=Gp*(tanpsi-sign(n0*dg)*n0)*(tanpsi-E*n)/(n-n0);
    G=Ge/(1+(Ge/Gplastic));
    G=max(10^(-30),(Ge/(1+Ge/Gplastic)));
    err=(tau-tauT);
    dg=(dg/(tau-tauT0))*(tauT-tauT0);
    chk=chk+1
    end
%%%%%%%%%%%%% inside of bounding surface %%%%%%%%%%%%%%%%%%%%%%%%%%
else
%%%%%%%%%%%%% dtermination of stiffness with old point %%%%%%%%%%%
    Ge=(Gn*(sn0/sn)^0.5);
    C=max(n,nrev);
    D=sign(dg);
    E=sign(nrev*dg);
    F=(n^2*(1-beta^m)/tanpsi^2);
    H=(C*sqrt(1-beta^m)/tanpsi);
    I=(tanpsi/sqrt(1-beta^m)-E*C);
    J=(1/abs(n-nrev+10^(-30)));
    Gplastic=lambda*((1-(D*F)*(1-H)))*I*J;
    G=max(10^(-20),(Ge/(1+Ge/Gplastic)));
    n1=n;

    while abs(err)>0.00001
    dn=G*dg;
    n=n1+dn;
    gdot=abs(dg)/dt*100*3600;
    M=theta*(sn0/snrev)^2;
    m = fzero(@(x) Sum(Suref,rho,gref,gdot,beta,tanpsi,x), m);
    sn=snrev*((tanpsi^2-n^2*(1-beta^m))/(tanpsi^2+(nrev^2-2*nrev*n)*(1-
beta^m)))^(1/M) ; %for n<tanpsi
    tau=(sn*n);
```

```
    Ge=(Gn*(sn0/sn)^0.5);
    C=max(n,nrev);
    D=sign(dg);
    E=sign(nrev*dg);
    F=(n^2*(1-beta^m)/tanpsi^2);
    H=(C*sqrt(1-beta^m)/tanpsi);
    I=(tanpsi/sqrt(1-beta^m)-E*C);
    J=(1/abs(n-nrev+10^(-30)));
    Gplastic=lambda*((1-(D*F)*(1-H)))*I*J;
    G=max(10^(-20),(Ge/(1+(Ge/Gplastic))));
    err=(tau-tauT);
    dg=((dg/(tau-tauT0))*(tauT-tauT0));
    chk=chk+1
    end
end
   g=g+dg;
   tauT0=tauT;
   ga=[ga,g];
   na=[na,n];
   sna=[sna,sn];
   taua=[taua, tau];
   gadot=[gadot, gdot];
end

 subplot(2,1,1)
 plot(sna,taua,':')
 hold on
 subplot(2,1,2)
 plot(ga,taua)
```

CYCLIC RESPONSE (STRAIN-CONTROLLED TEST)

```
clear all
clf

%%%%%%%% Set up the material parameters %%%%%%%%%%%%%%%%%%%
beta=0.32;
m=0.1;
psi=28;
Gn=450;
Gp=12;

theta=10;
lambda=7;
%%%%%%%%%%%%%%%%%%%%%%%%%%%%%%%%%%%%%%%%%%%%%%%%%%%%%%%%%%%%
tanpsi=tan(psi*pi/180);
A= sqrt(1/((1-beta^m)*(1+2/m)));
Suref= A*(2/(2+m))^(1/m)*tanpsi;

rho=0.077;
gref=5;

one_b=1-beta^m;
bm=beta^m;
mparam=[beta,tanpsi,one_b,bm,rho,gref,Suref];

%%%%%%% set up initial condition %%%%%%%%%%%%%%%%%%%%%%%

sn0=1.0;
tau0=0.0;
g0=0.0;
n0=tau0/sn0;
nrev=n0;
snrev=sn0;
dir=1;
Ga=0;
Gpla=0;
N=0;
taut=0;
t=0;


na=[n0];
ga=[g0];
sna=[sn0];
taua=[tau0];
gadot=[];
n=n0;
g=g0;
sn=sn0;
```

```
tau=tau0;
tauT1=[tau0];
tauT0=tau0;
dga=[0];

%%%%%%%%% set up cyclic load, sine wave for shear stress %%%%%%%
rate=100/3600;
T=10; % period of the sine wave in second
% N=1;
space=100;
dt=T/space;

t=dt;
chk=0;
dir=1;
nsurf=1;

%%%%%%% First step to avoid divide by zero on first load %%%%%%%%
t=t+dt;
gamma=rate*sin(2*pi*t/T);
N=t/T;
dg=gamma-g0;

Ge=Gn*(sn0/sn)^0.5;
E=sign(n0*dg);
Gplastic=Gp*(tanpsi-sign(n0*dg)*n0)*(tanpsi-E*n0)/(n0-n0+10^(-
30))+10^(-30);
G=max(10^(-30),(Ge/(1+(Ge/Gplastic))));

dn=Ge*dg;
n=n0+dn;
sn= sn0*(beta^m+((1-beta^m)*(tanpsi^2-n^2)/(tanpsi^2+0.8*n0^2-
1.8*n0*n)))^(1/m);
tau=sn*n;

g=g+dg;
ga=[ga,g];
na=[na,n];
sna=[sna,sn];
taua=[taua, tau];
dga=[dga,dg];

for k=2:2500   %number of data points
    t=t+dt;
    gamma=rate*sin(2*pi*t/T);
    N=t/T;
    err=0.1;
    dg=gamma-g;
    n1=n;
%%%%%% determination of reversal point(nrev and snrev)%%%%%%%%%%
    if abs(gamma)>=(rate+tau0) | (gamma)<=(tau0-rate)
        nrev=n;
```

```
        snrev=sn;
    end
 %%%%%%%%%%%%%%%%%%%%%%%%%%%%%%%%%%%%%%%%%%%%%%%%%%%%%%%%%%%%%%%%%%%

%%%%%%%%% on plastic bounding surface %%%%%%%%%%%%%%%%%%%%%%%%%%%%
if N<=0.249

    E=sign(n1*dg);
    Ge=Gn*(sn0/sn)^0.5;
    Gplastic=Gp*(tanpsi-sign(n0*dg)*n0)*(tanpsi-E*n1)/(n1-n0);
    G=max(10^(-30),(Ge/(1+(Ge/Gplastic))));
    dn=G*dg;
    n=n1+dn;
    sn= sn0*(beta^m+(1-beta^m)*(tanpsi^2-n^2)/(tanpsi^2+0.8*nrev^2-
1.8*nrev*n))^(1/m);
    tau=sn*n;

%%%%%%%%%%%%%%%%%%%%%%%%%%%%%%%%%%%%%%%%%%%%%%%%%%%%%%%%%%%%%%%%%%%
%%%%%%%%%%%%% inside of bounding surface %%%%%%%%%%%%%%%%%%%%%%%%%
else
%%%%%%%%%%%%% dtermination of stiffness with old point %%%%%%%%%%%
    Ge=(Gn*(sn0/sn)^0.5);
    C=max(n1,nrev);
    D=(n1*dg);
    E=(nrev*dg);
    F=(n1^2*(1-beta^m)/tanpsi^2);
    H=(C*sqrt(1-beta^m)/tanpsi);
    I=(tanpsi/sqrt(1-beta^m)-(E)*C);
    J=(1/abs(n1-nrev+10^(-20)));
    Gplastic=lambda*((1-((D)*F)*(1-H)))*I*J;
    G=max(10^(-20),(Ge/(1+Ge/Gplastic)));
    dn=G*dg;
    n=n1+dn;
    M=theta*(sn0/snrev)^2;
    sn=snrev*((tanpsi^2-n^2*(1-beta^m))/(tanpsi^2+(nrev^2-2*nrev*n)*(1-
beta^m)))^(1/M) ; %for n<tanpsi
    tau=(sn*n);

end
   g=g+dg;
   ga=[ga,g];
   na=[na,n];
   sna=[sna,sn];
   taua=[taua, tau];
end

 subplot(2,1,1)
 plot(ta,taua,':')
 hold on
 subplot(2,1,2)
 plot(ga,taua)
```

VITA

Byoung Chan, Jung was born on August 20, 1975 in Korea. During 1994-1997 he served his country in the division of operation, 98^{th} battalion, 5^{th} Artillery brigade, the Republic of Korea Army. He enrolled at Tae Jeon University, in Tae Jeon, South Korea, where he received a Bachelor of Engineering degree in civil engineering in 2000. In the fall of 2002, he enrolled in the Department of Civil Engineering at Texas A&M University in order to pursue the M.S degree. He received his M.S degree in May 2005. He is interested in dynamic response and constitutive modeling cohesive materials.

His permanent mailing address is:

262-2 Asan-Ri
Young-In-Myun, Asan-Si
Chung-Nam, Korea